Supporting Information For:

Multi-color solid-state emission of β-iminoenolate boron complexes tuned by methoxyl group: Aggregation-induced emission and mechanofluorochromism

Zhenqi Zhang, Zhu Wu, Jingbo Sun, Pengchong Xue and Ran Lu*

State Key Laboratory of Supramolecular Structure and Materials, College of Chemistry,

Jilin University, Changchun 130012, P. R. China

Fax: +86-431-88923907; Tel: +86-431-88499179

E-Mail: luran@mail.jlu.edu.cn

Table S1. Photophysical properties of β-iminoenolate boron complexes in solution.

Compound	Solvents	λ_{abs}[a]	λ_{em}[a]	Stokes shift (cm^{-1})	Φ_F[b]
BB	Cyclohexane	351(39911)	410	4100	0.01
	Toluene	355(35400)	428	4805	0.01
	THF	352(39854)	425	4880	0.01
	DCM	351(39659)	430	5234	0.01
	DMF	352(36760)	427	4990	0.01
B2B	Cyclohexane	355(47654), 369(46107)	409	3719	0.01
	Toluene	359(42167), 372(42695)	430	3626	0.01
	THF	358(39913), 371(40282)	425	3425	0.01
	DCM	358(44032), 371(44766)	428	3590	0.01
	DMF	360(41248), 371(42056)	425	3425	0.01
B3B	Cyclohexane	355(30268)	409	3719	0.01
	Toluene	357(40127)	430	4755	0.01
	THF	355(37232)	427	4750	0.01
	DCM	355(44016)	427	4750	0.01
	DMF	356(42415)	427	4671	0.01
B4B	Cyclohexane	360(36907), 370(35739)	426	4304	0.02
	Toluene	363(46425), 374(46049)	433	4453	0.02
	THF	362(48707), 371(48064)	430	4368	0.02
	DCM	361(51712), 373(50802)	430	4445	0.02
	DMF	363(47760), 375(47763)	433	3572	0.03
B24B	Cyclohexane	374(38344)	426	3264	0.02
	Toluene	378(47020)	433	3360	0.03
	THF	378(50606)	431	3253	0.03
	DCM	378(49495)	433	3360	0.03
	DMF	378(47045)	437	3572	0.04
B25B	Cyclohexane	345(22374), 379(29834)	431	3183	0.02
	Toluene	347(18884), 385(26292)	444	3451	0.06
	THF	346(25641), 381(32513)	453	4172	0.08
	DCM	346(21689), 383(27400)	456	4180	0.11
	DMF	347(20239), 383(24617)	474	5013	0.29
B345B	Cyclohexane	365(33488)	433	4303	0.03
	Toluene	366(36134)	444	4800	0.04
	THF	365(26825)	442	4773	0.04
	DCM	364(39444)	444	4950	0.03
	DMF	368(37615)	446	4752	0.06

[a] The maximum absorption and fluorescence emission wavelength in solution (1×10^{-5} M), [b] The fluorescence quantum yield (Φ_F) was measured using quinine sulfate in H_2SO_4 (0.1 M) ($\Phi_F = 0.55$) as standard.

Table S2. Emitting properties of β-iminoenolate boron complexes in THF and aggregation states.

	In THF		In THF/H_2O		In solid	
	λ_{em}^{a} (nm)	Φ_F^{b}	λ_{em}(nm) (%)^c	I/I_0	λ_{em}^{d} (nm)	λ_{em}^{e} (nm)
BB	425	0.01	468 (90)	44	478	476
B2B	425	0.01	436,459 (95)	91	439	461
B3B	427	0.01	471 (80)	48	462	473
B4B	430	0.02	480,550 (90)	12	480, 550	480, 550
B24B	431	0.03	476 (95)	11	471	470
B25B	453	0.08	476 (80)	1.2	466	500
B345B	442	0.04	500 (90)	2.6	505	512

[a] The maximum fluorescence emission wavelength in THF solution (1×10^{-5} M), [b] The fluorescence quantum yield (Φ_F) in THF using quinine sulfate in H_2SO_4 (0.1M) (Φ_F = 0.55) as standard, [c] The maximum emission intensity in THF/H_2O and the corresponding water content, [d] The maximum emission wavelength of the as-synthesized powder, [e] The maximum emission wavelength of the single crystal.

Table S3. Fluorescence lifetimes of **B4B** in solutions and in solid states.

State	Wavelength (nm)	Lifetime (ns)
In THF	430	0.48
In THF/H_2O (v/v = 2/8)	480	18.54
In THF/H_2O (v/v = 1/9)	480	13.28
	550	23.68
Crystal	480	10.47
	550	16.89
Ground powder 1	505	14.87
Ground powder 2	450	3.20

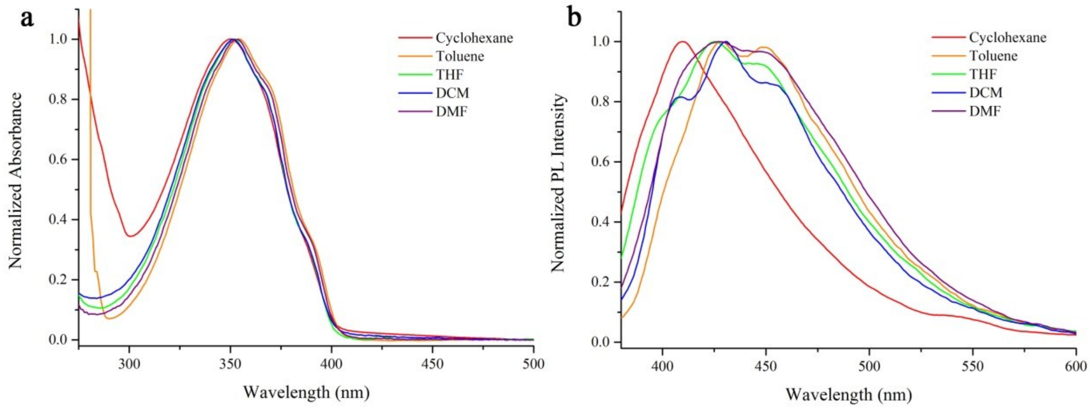

Figure S1. Normalized UV-vis (a) and PL spectra (b) (λ_{ex} = 365 nm) of **BB** in different solvents (1×10^{-5} mol/L).

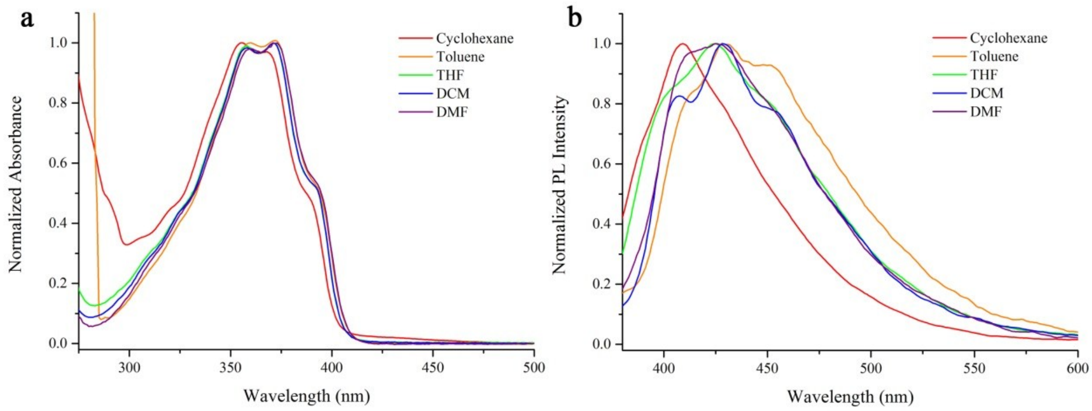

Figure S2. Normalized UV-vis (a) and PL spectra (b) (λ_{ex} = 365 nm) of **B2B** in different solvents (1×10^{-5} mol/L).

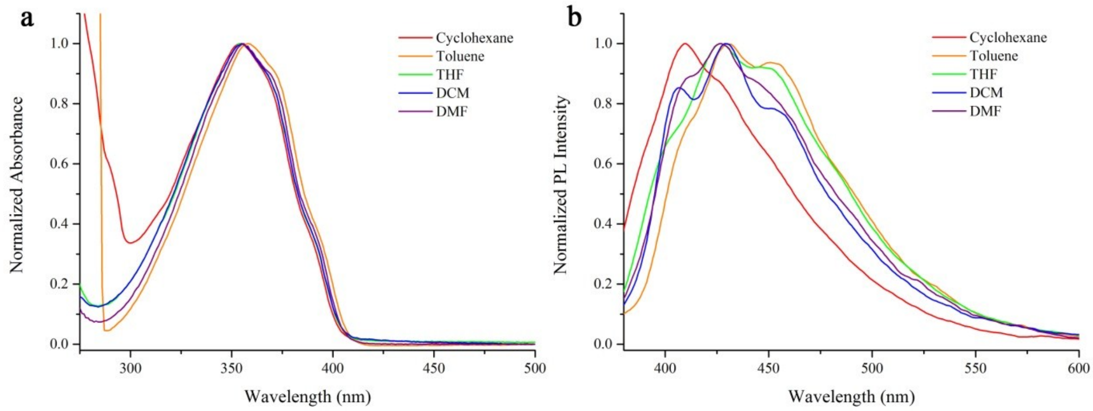

Figure S3. Normalized UV-vis (a) and PL spectra (b) (λ_{ex} = 365 nm) of **B3B** in different solvents (1×10^{-5} mol/L).

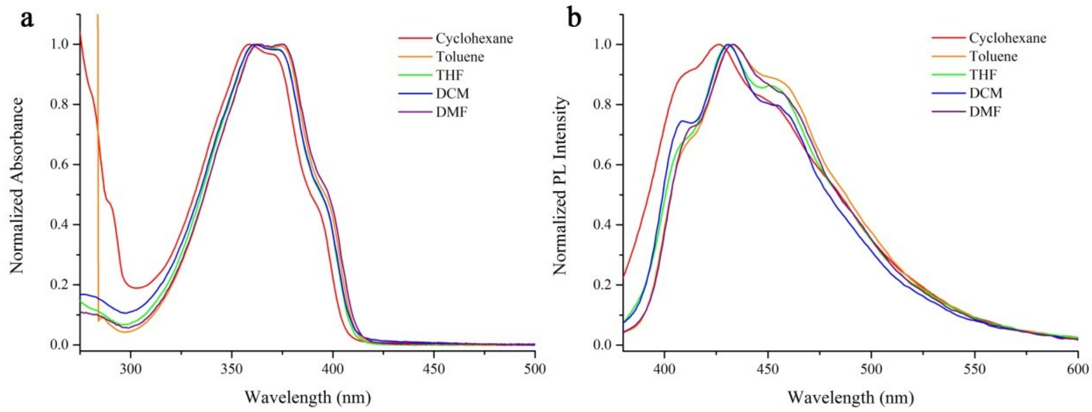

Figure S4. Normalized UV-vis (a) and PL spectra (b) (λ_{ex} = 365 nm) of **B4B** in different solvents (1×10^{-5} mol/L).

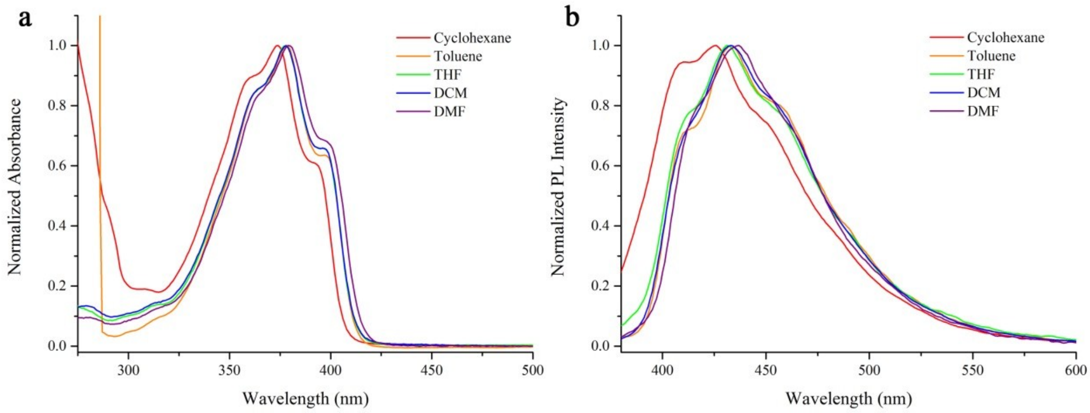

Figure S5. Normalized UV-vis (a) and PL spectra (b) (λ_{ex} = 365 nm) of **B24B** in different solvents (1×10^{-5} mol/L).

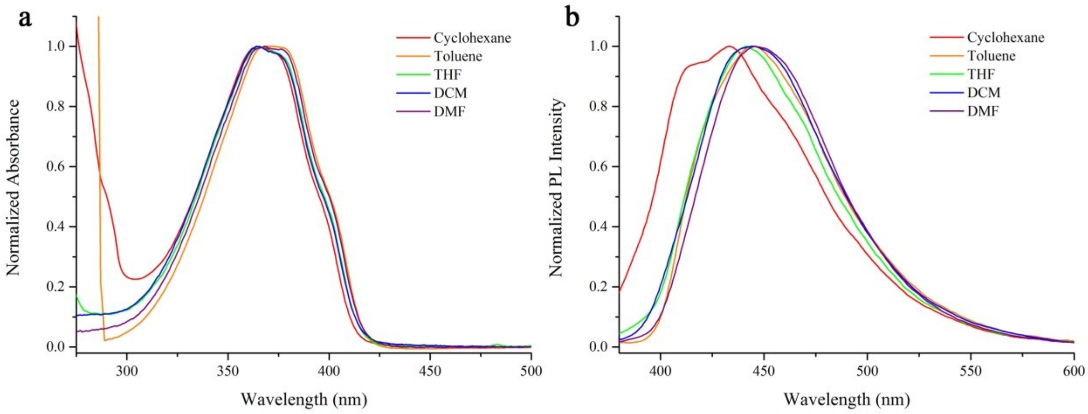

Figure S6. Normalized UV-vis (a) and PL spectra (b) (λ_{ex} = 365 nm) of **B345B** in different solvents (1×10^{-5} mol/L).

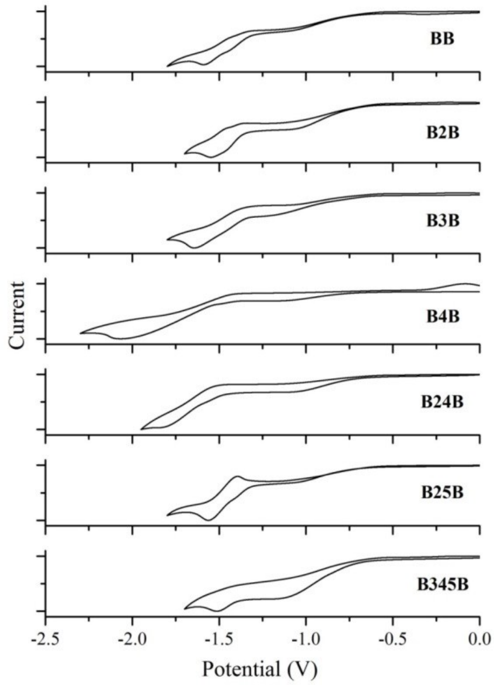

Figure S7. Cyclic voltammograms of **BB**, **B2B**, **B3B**, **B4B**, **B24B**, **B25B** and **B345B** measured in CH_2Cl_2 with Bu_4NBF_4 (0.1 M) as electrolyte at a scan rate of 50 mV/s .

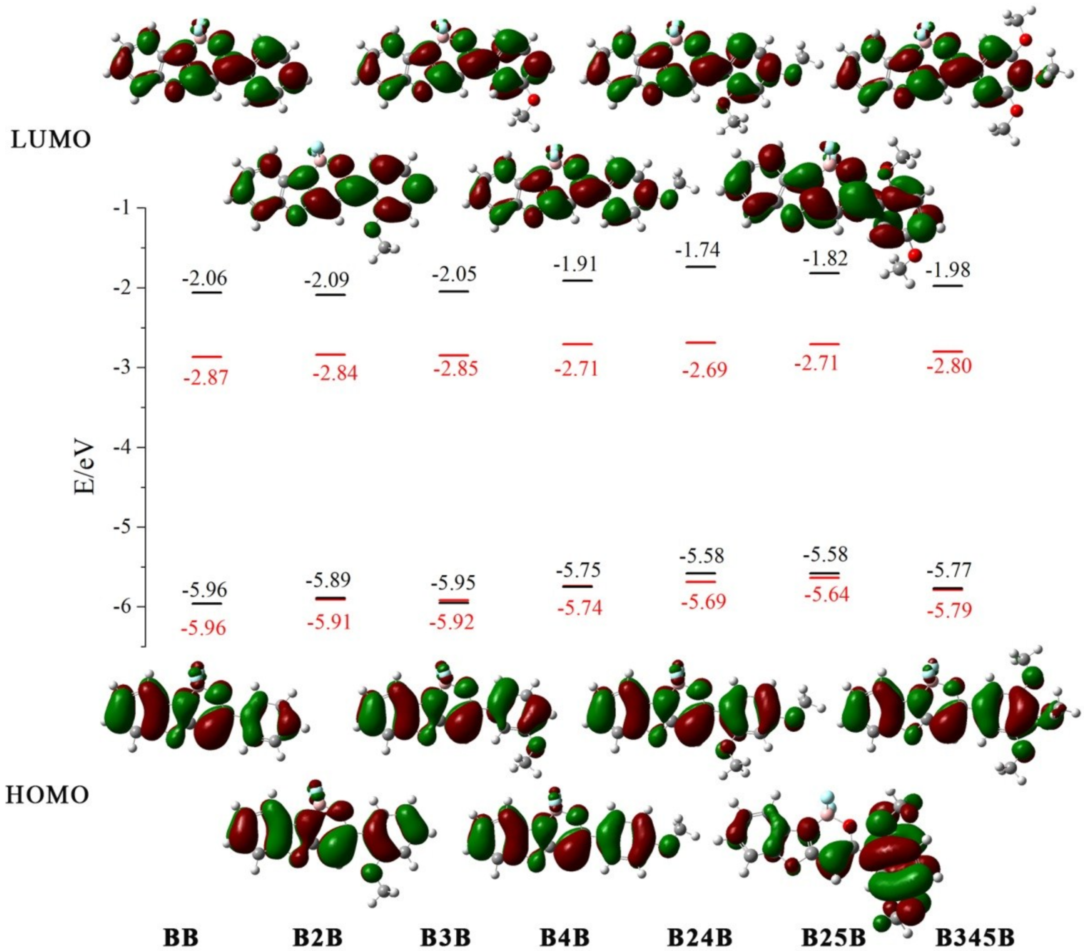

Figure S8. The frontier orbital plots of the HOMO/LUMO and the energy levels of the HOMO/LUMO obtained using electrochemical method (red) and DFT calculation (black).

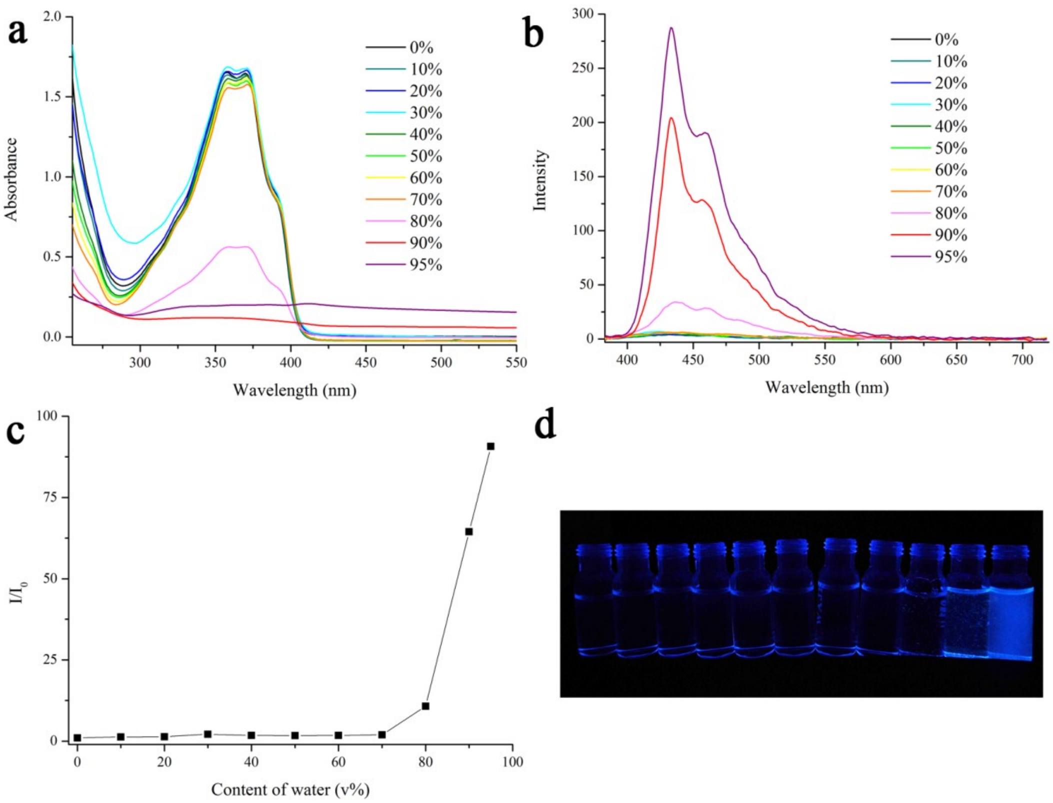

Figure S9. (a) UV-vis absorption and (b) fluorescence emission spectra (λ_{ex} = 365 nm) of **B2B** (5 × 10^{-5} M) in THF/H_2O with different amounts of water (% volume), (c) a plot of PL integral versus water content of the solvent mixture for **B2B** and (d) photograph of **B2B** (5 × 10^{-5} M) in THF/H_2O with different contents of water (0, 10, 20, 30, 40, 50, 60, 70, 80, 90, 95%) under UV light.

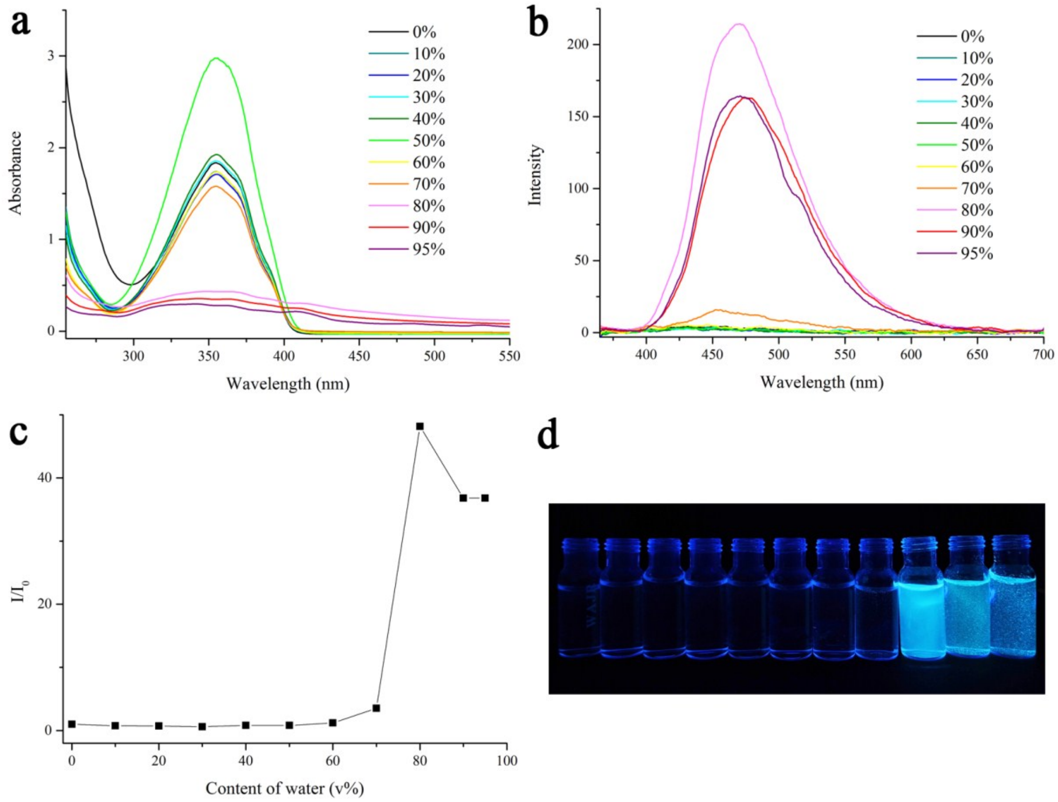

Figure S10. (a) UV-vis absorption and (b) fluorescence emission spectra (λ_{ex} = 365 nm) of **B3B** (5×10^{-5} M) in THF/H_2O with different amounts of water (% volume), (c) a plot of PL integral versus water content of the solvent mixture for **B3B** and (d) photograph of **B3B** (5×10^{-5} M) in THF/H_2O with different contents of water (0, 10, 20, 30, 40, 50, 60, 70, 80, 90, 95%) under UV light.

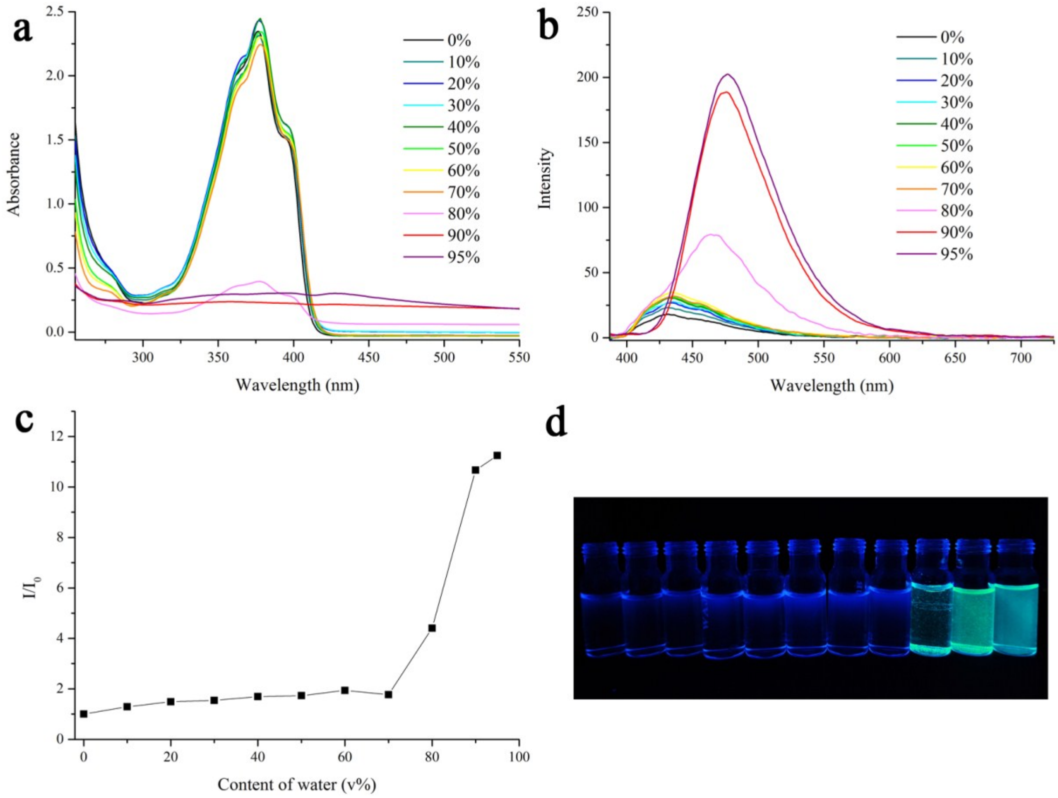

Figure S11. (a) UV-vis absorption and (b) fluorescence emission spectra (λ_{ex} = 365 nm) of **B24B** (5×10^{-5} M) in THF/H_2O with different amounts of water (% volume), (c) a plot of PL integral versus water content of the solvent mixture for **B24B** and (d) photograph of **B24B** (5×10^{-5} M) in THF/H_2O with different contents of water (0, 10, 20, 30, 40, 50, 60, 70, 80, 90, 95%) under UV light.

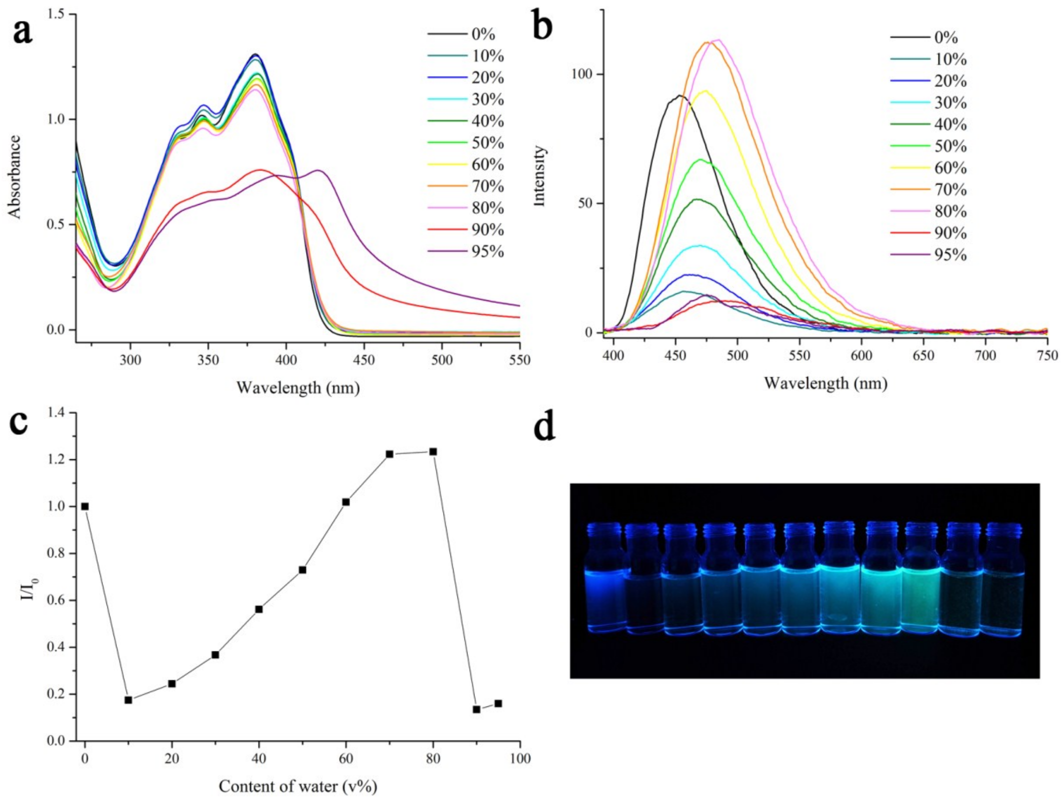

Figure S12. (a) UV-vis absorption and (b) fluorescence emission spectra (λ_{ex} = 365 nm) of **B25B** (5×10^{-5} M) in THF/H_2O with different amounts of water (% volume), (c) a plot of PL integral versus water content of the solvent mixture for **B25B** and (d) photograph of **B25B** (5×10^{-5} M) in THF/H_2O with different contents of water (0, 10, 20, 30, 40, 50, 60, 70, 80, 90, 95%) under UV light.

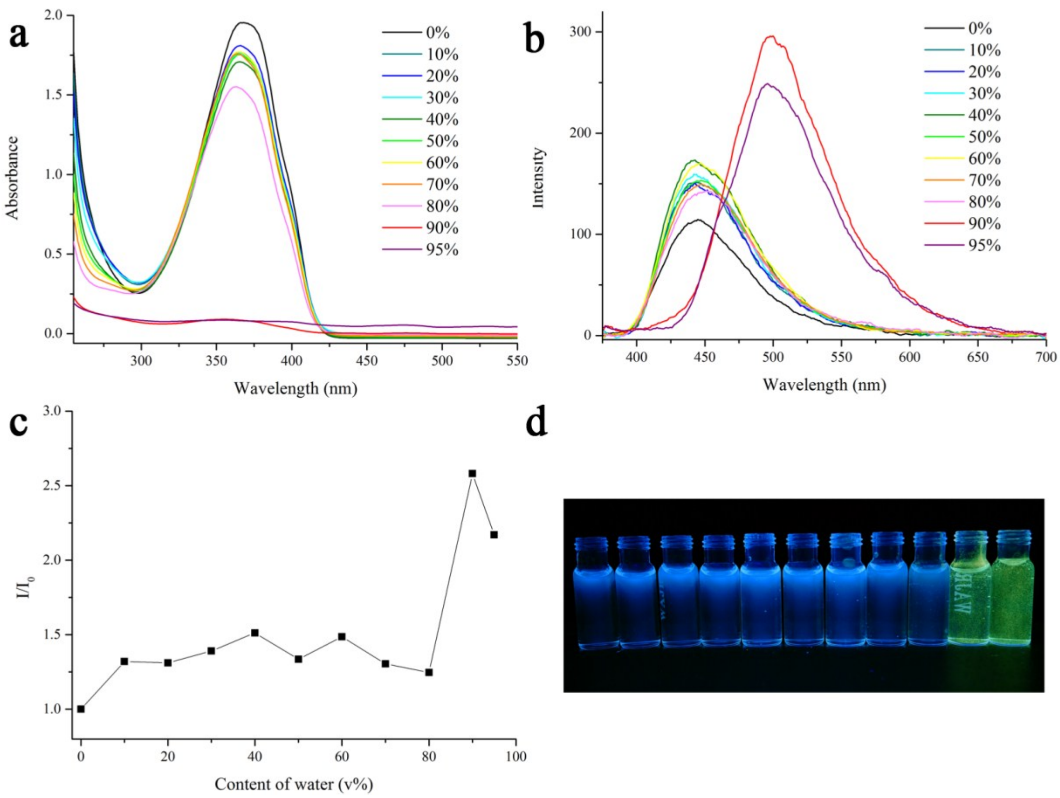

Figure S13. (a) UV-vis absorption and (b) fluorescence emission spectra (λ_{ex} = 365 nm) of **B345B** (5×10^{-5} M) in THF/H_2O with different amounts of water (% volume), (c) a plot of PL integral versus water content of the solvent mixture for **B345B** and (d) photograph of **B345B** (5×10^{-5} M) in THF/H_2O with different contents of water (0, 10, 20, 30, 40, 50, 60, 70, 80, 90, 95%) under UV light.

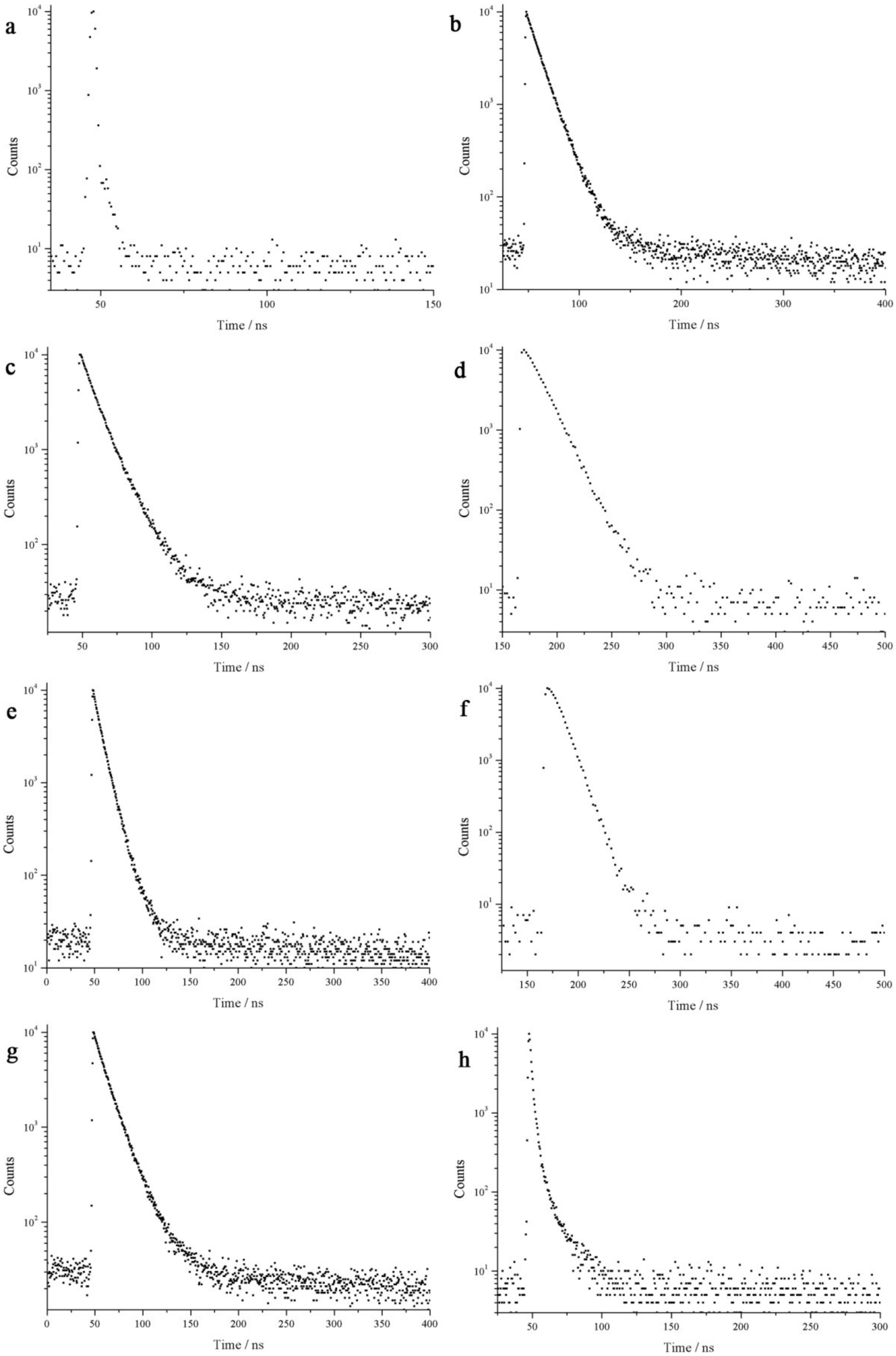

Figure S14. Time-resolved emission decay curves of **B4B** in THF monitored at 430 nm (a); in THF/H_2O (v/v = 2/8) monitored at 480 nm (b); in THF/H_2O (v/v = 1/9) monitored at 480 nm (c); in THF/H_2O (v/v = 1/9) monitored at 550 nm (d); in crystal state monitored at 480 nm (e); in crystal state monitored at 550 nm (f); in ground powder 1 monitored at 505 nm (g) and in ground powder 2 monitored at 450 nm (h).

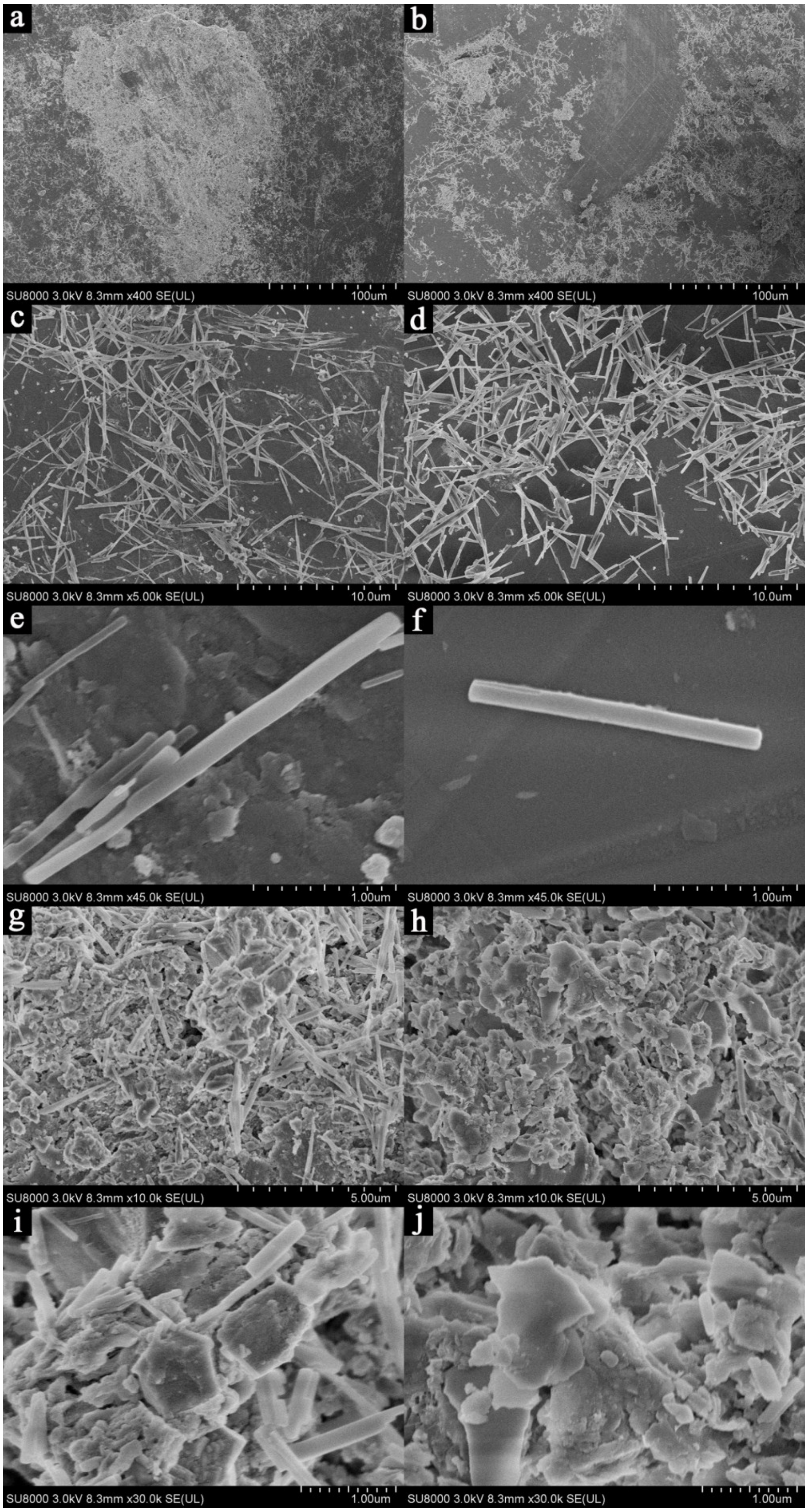

Figure S15. SEM images of the aggregates gained from **B4B** in THF/H_2O with water content of 80% (a) and 90% (b); SEM images of the fibres generated from **B4B** in THF/H_2O with water content of 80% (c, e) and 90% (d, f); SEM images of the blocky structures generated from **B4B** in THF/H_2O with water content of 80% (g, i) and 90% (h, j).

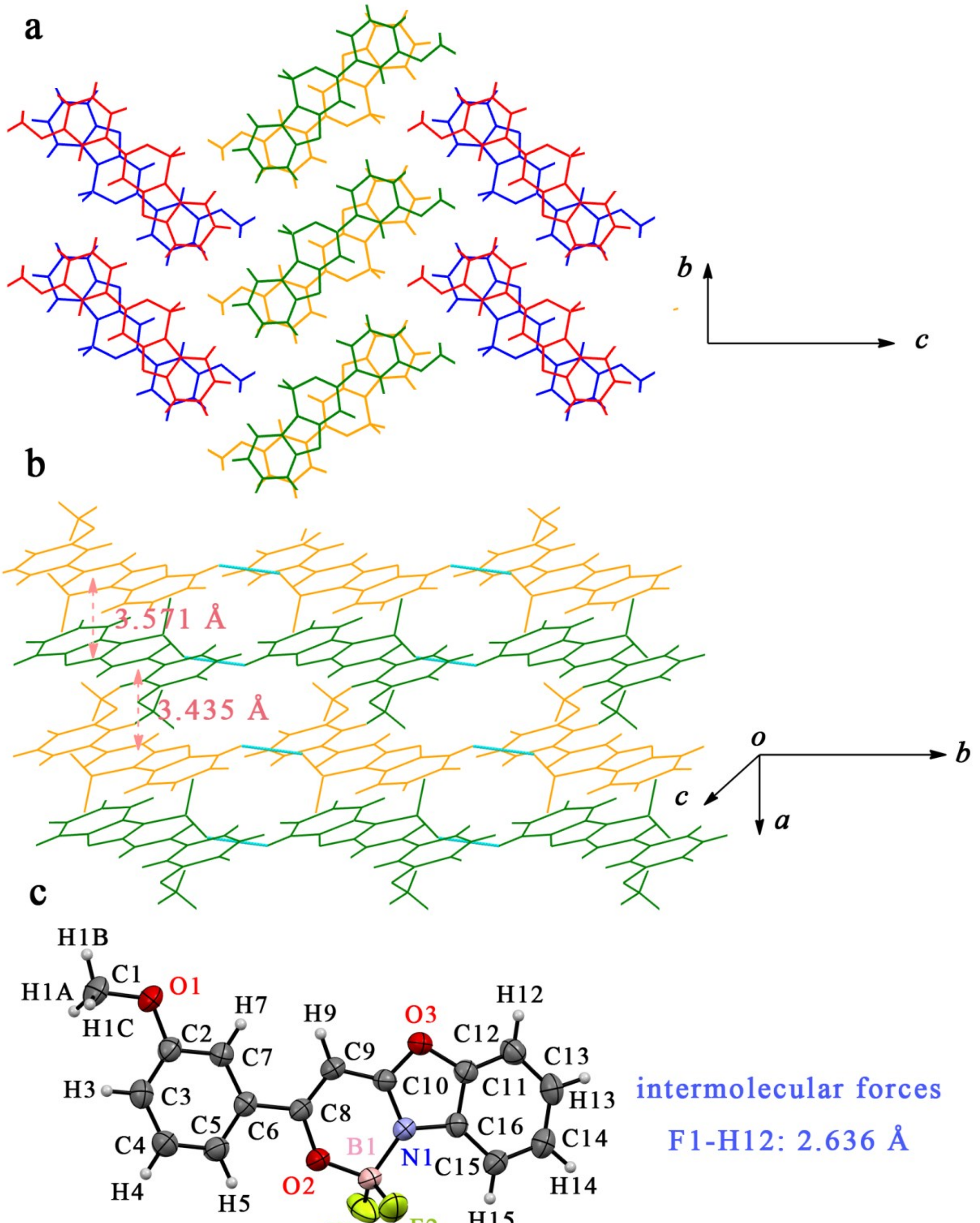

Figure S16. (a) Crystal structure of **B3B** viewed along *a* axis; (b) crystal structure of **B3B**, intermolecular forces (blue line) and distances between molecules (pink arrow); (c) ORTEP view and list of intermolecular forces.

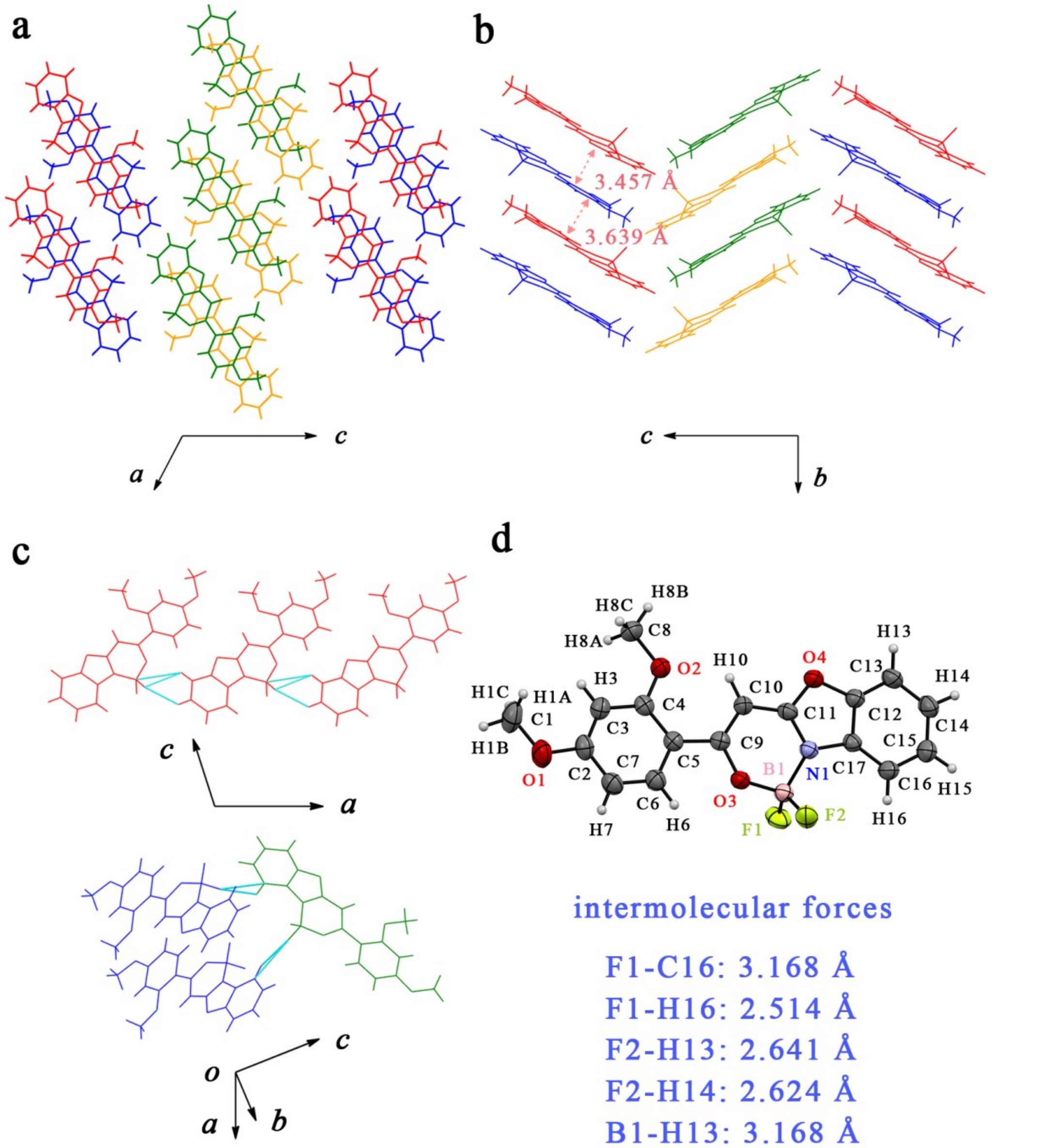

Figure S17. (a) Crystal structure of **B24B** viewed along *b* axis; (b) crystal structure of **B24B** viewed along *a* axis, intermolecular forces (blue line) and distances between molecules (pink arrow); (c) ORTEP view and list of intermolecular forces.

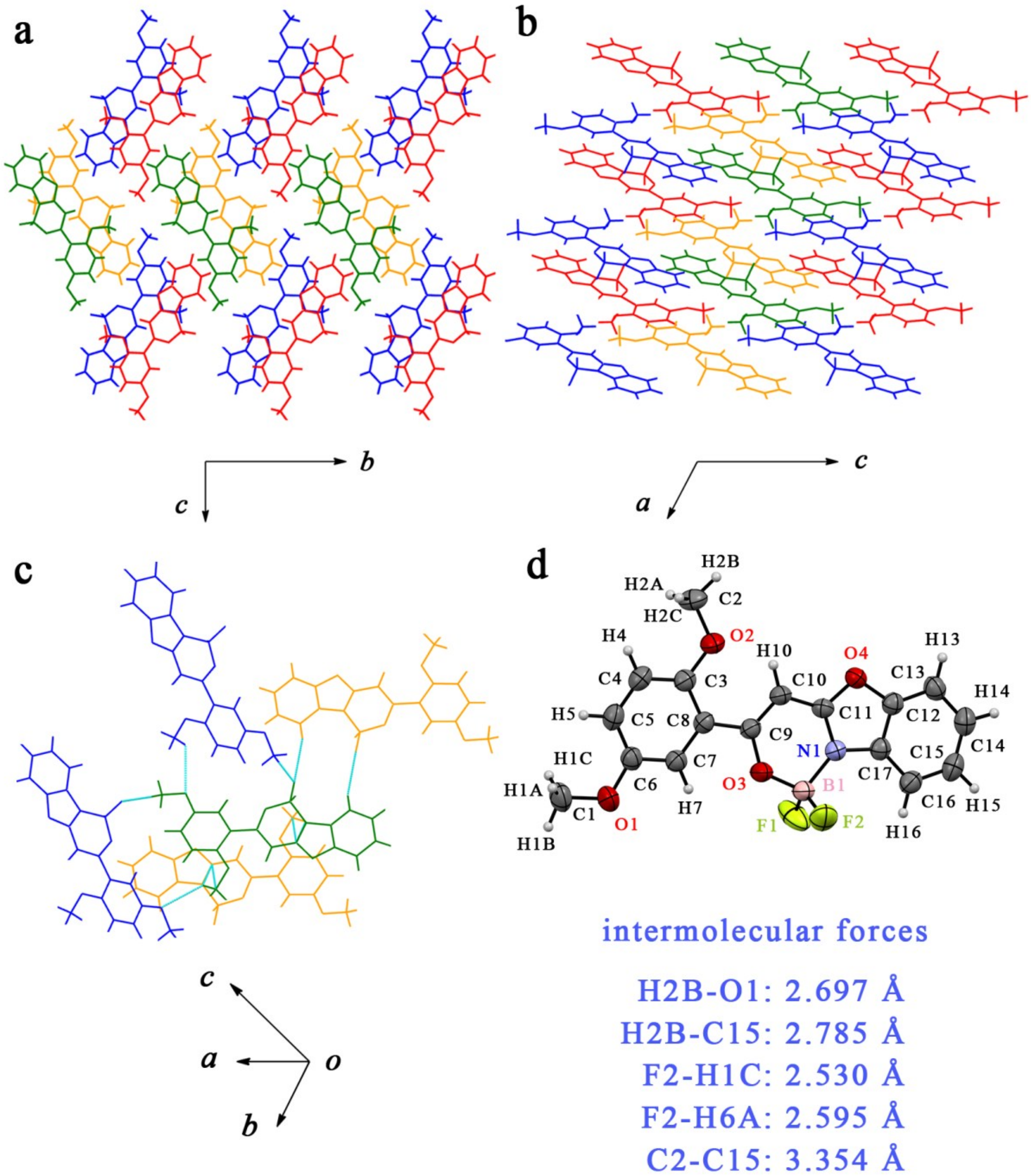

Figure S18. (a) Crystal structure of **B25B** viewed along *a* axis; (b) crystal structure of **B25B** viewed along *b* axis; (c) intermolecular forces (blue line); (d) ORTEP view and list of intermolecular forces.

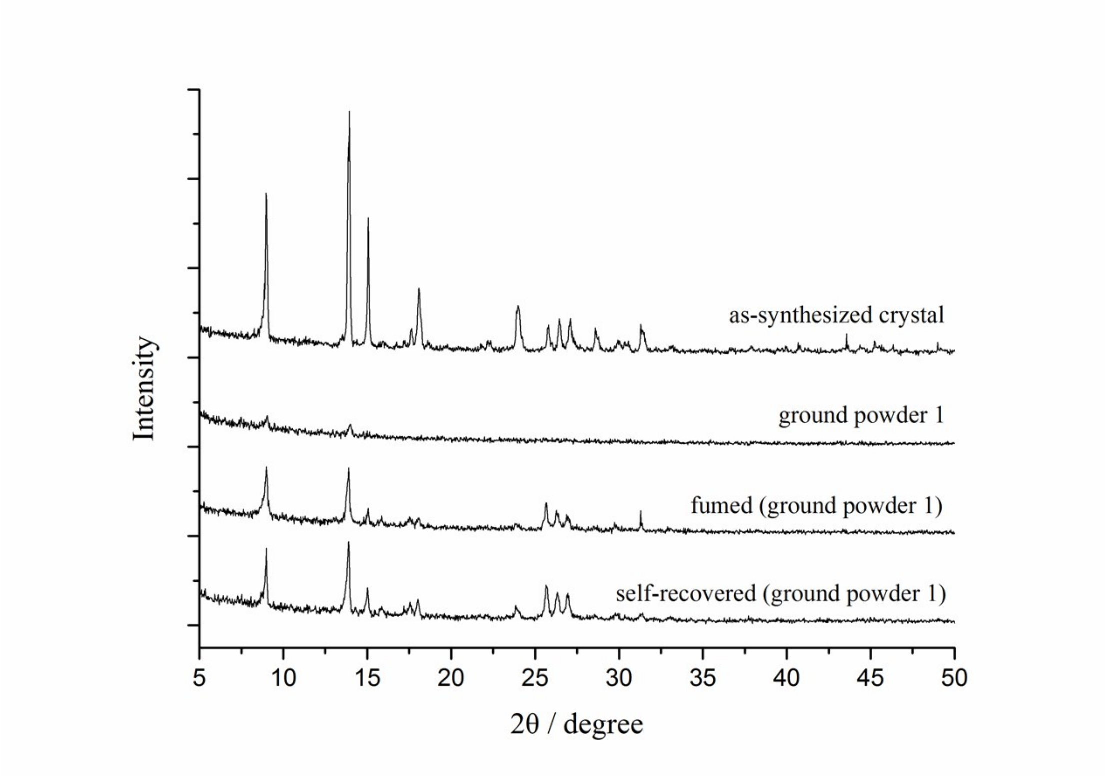

Figure S19. XRD patterns of **B4B** in different solid states.

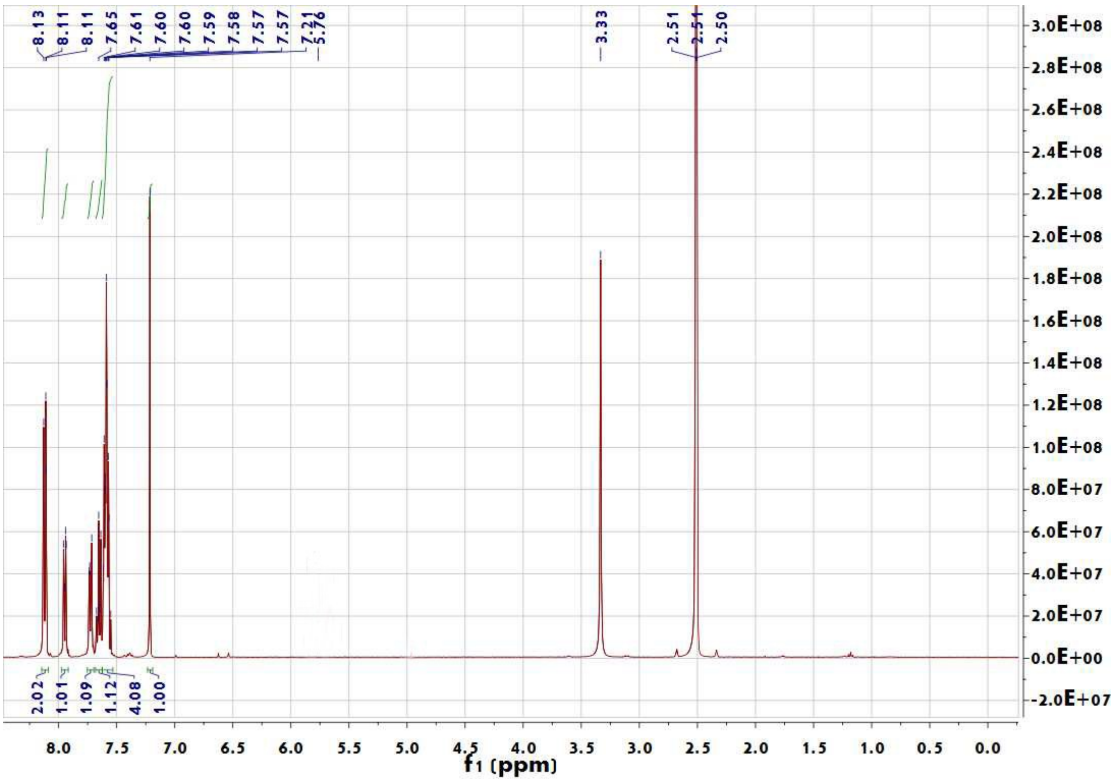

Figure S20. ^{1}H NMR (400 MHz) spectrum of compound **BB** in DMSO-d_6

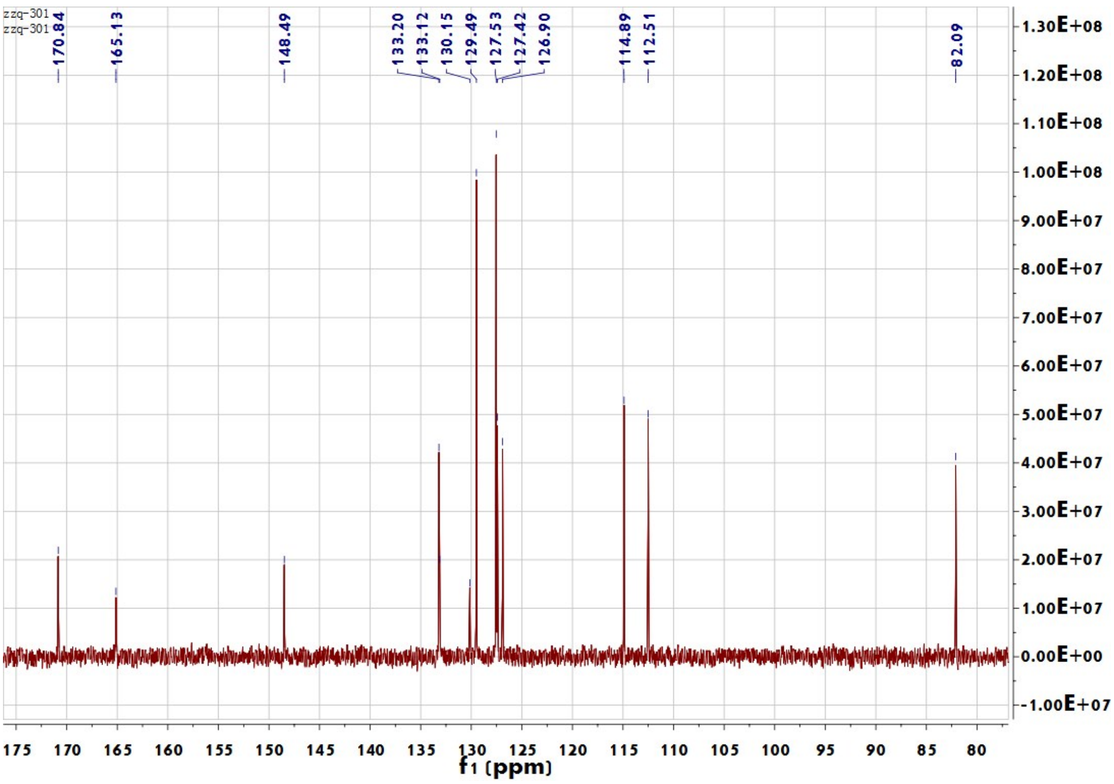

Figure S21. ^{13}C NMR (100 MHz) spectrum of compound **BB** in DMSO-d_6

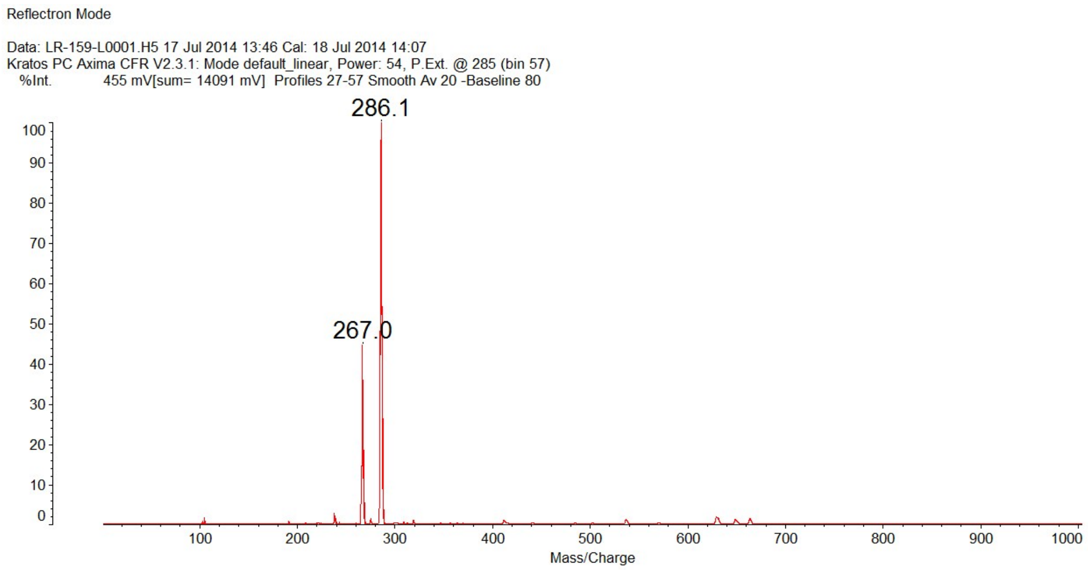

Figure S22. MALDI/TOF MS spectrum of compound **BB**.

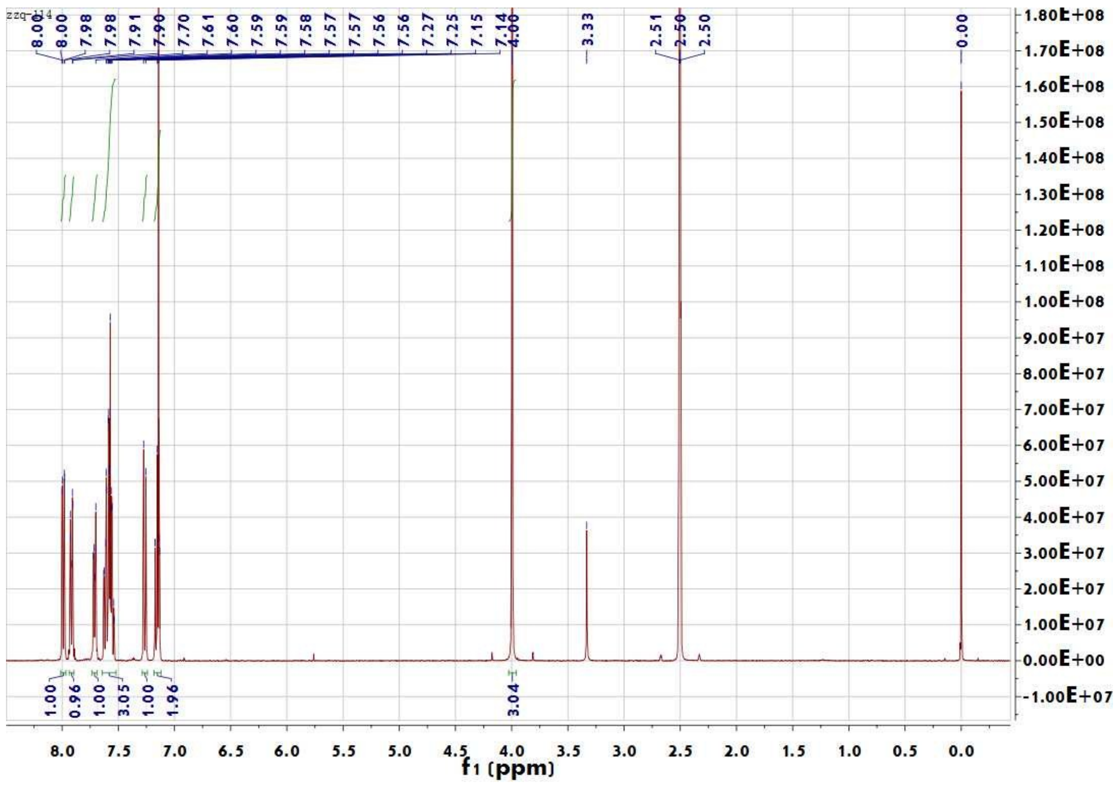

Figure S23. ^{1}H NMR (400 MHz) spectrum of compound **B2B** in DMSO-d_6

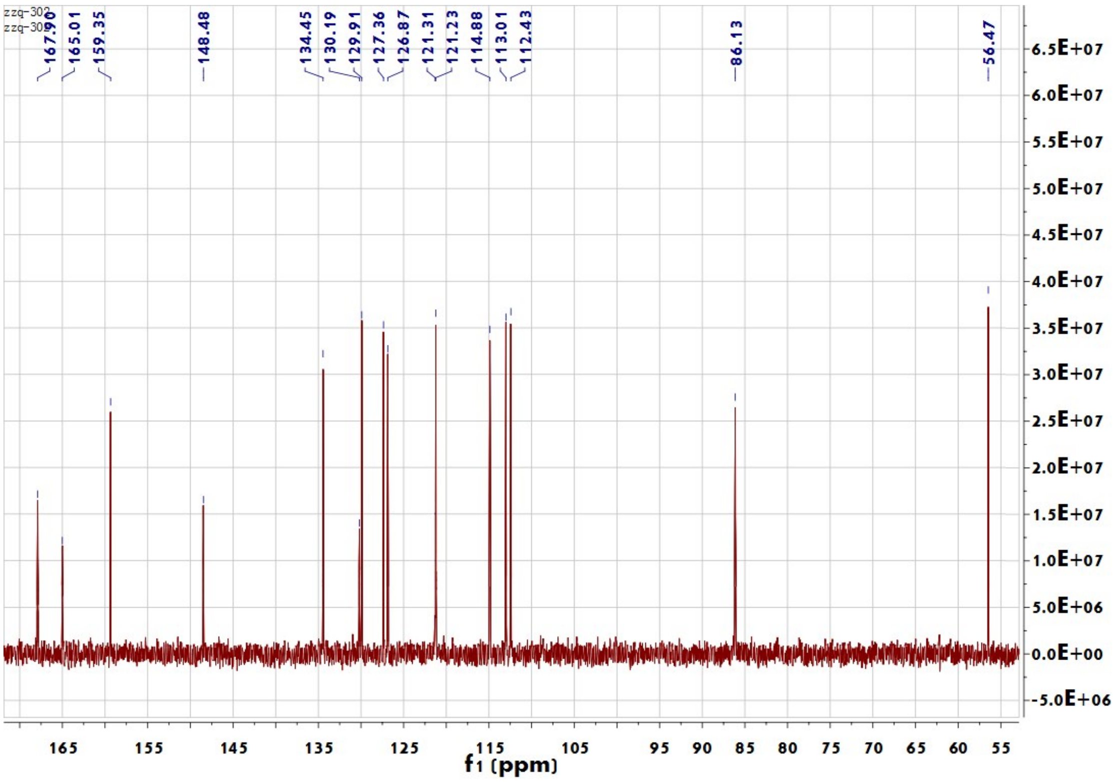

Figure S24. ^{13}C NMR (100 MHz) spectrum of compound **B2B** in DMSO-d_6

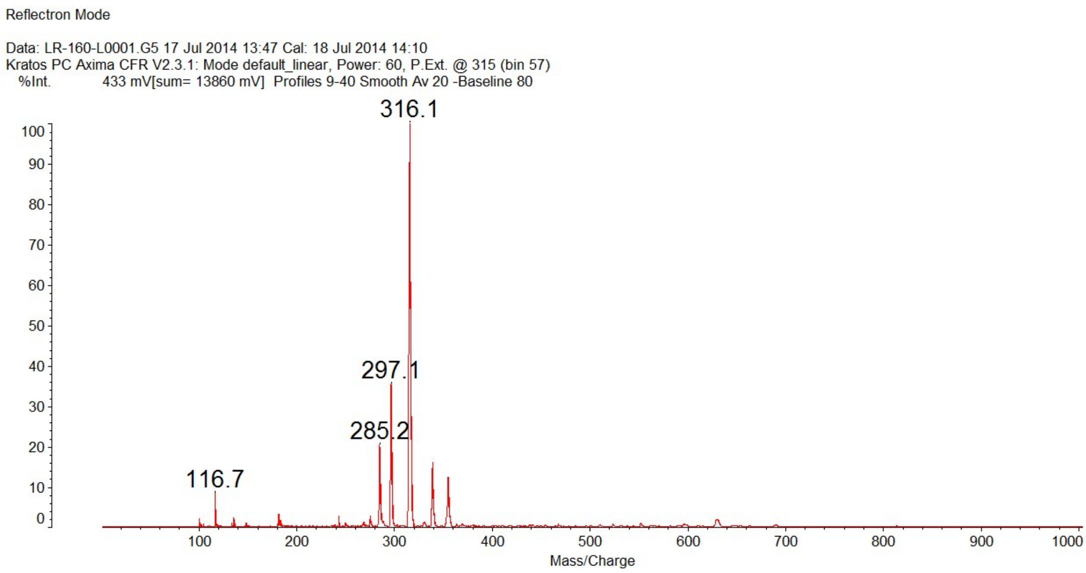

Figure S25. MALDI/TOF MS spectrum of compound **B2B**

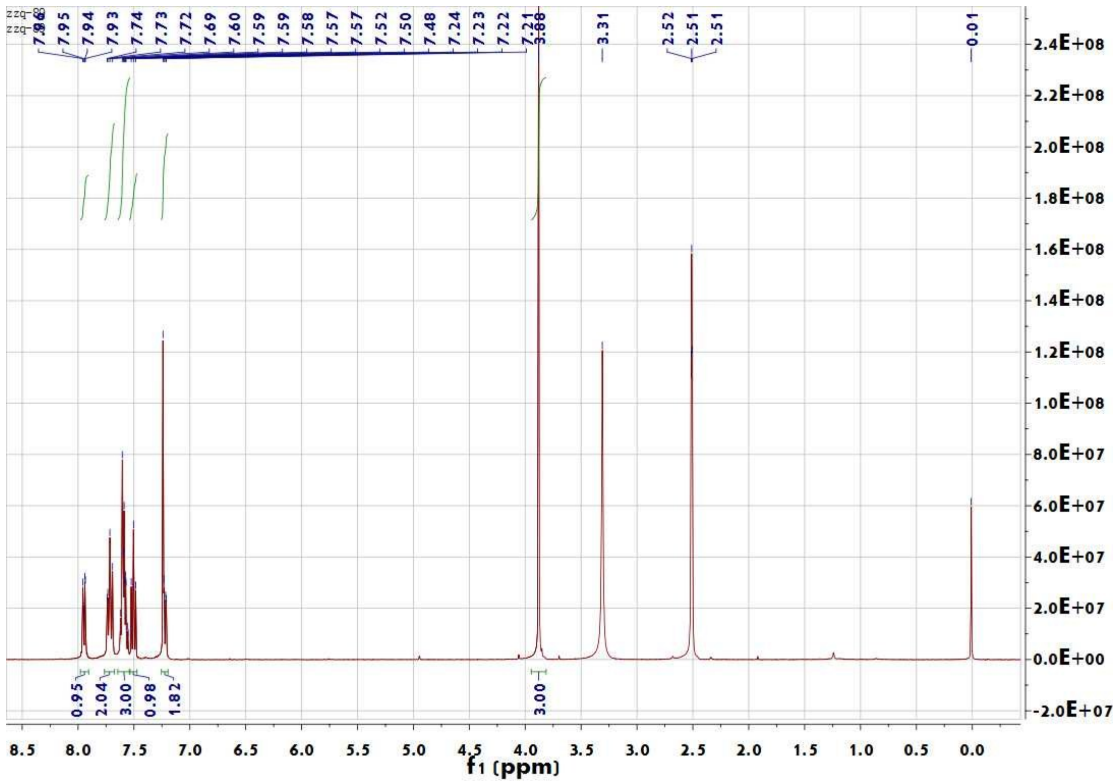

Figure S26. ^{1}H NMR (400 MHz) spectrum of compound **B3B** in DMSO-d_6

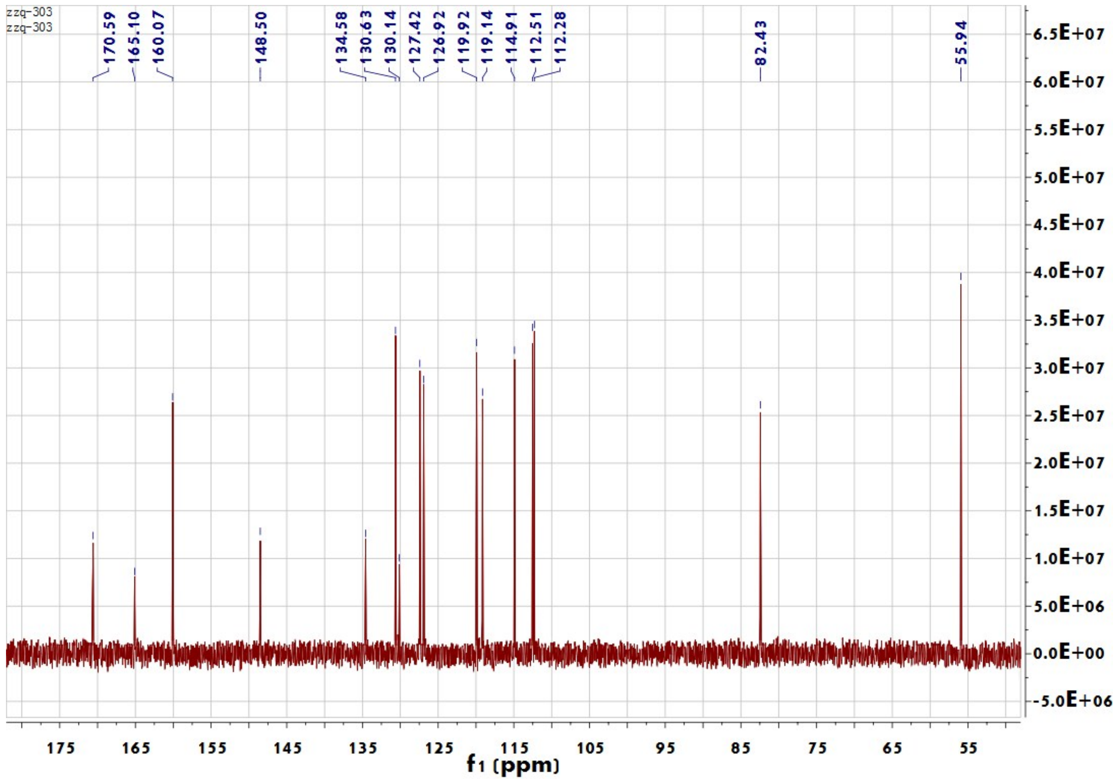

Figure S27. ^{13}C NMR (100 MHz) spectrum of compound **B3B** in DMSO-d_6

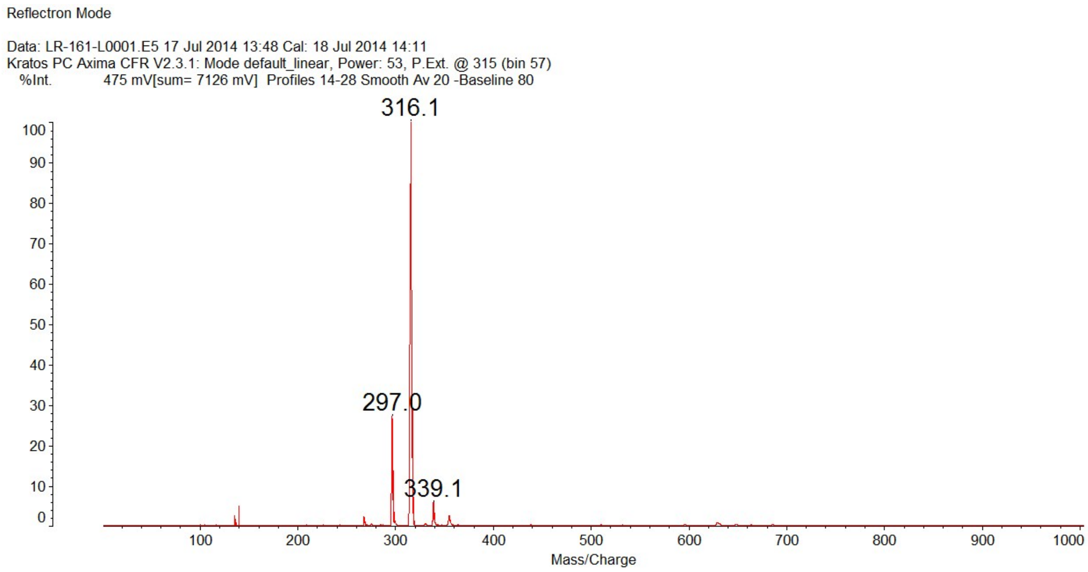

Figure S28. MALDI/TOF MS spectrum of compound **B3B**.

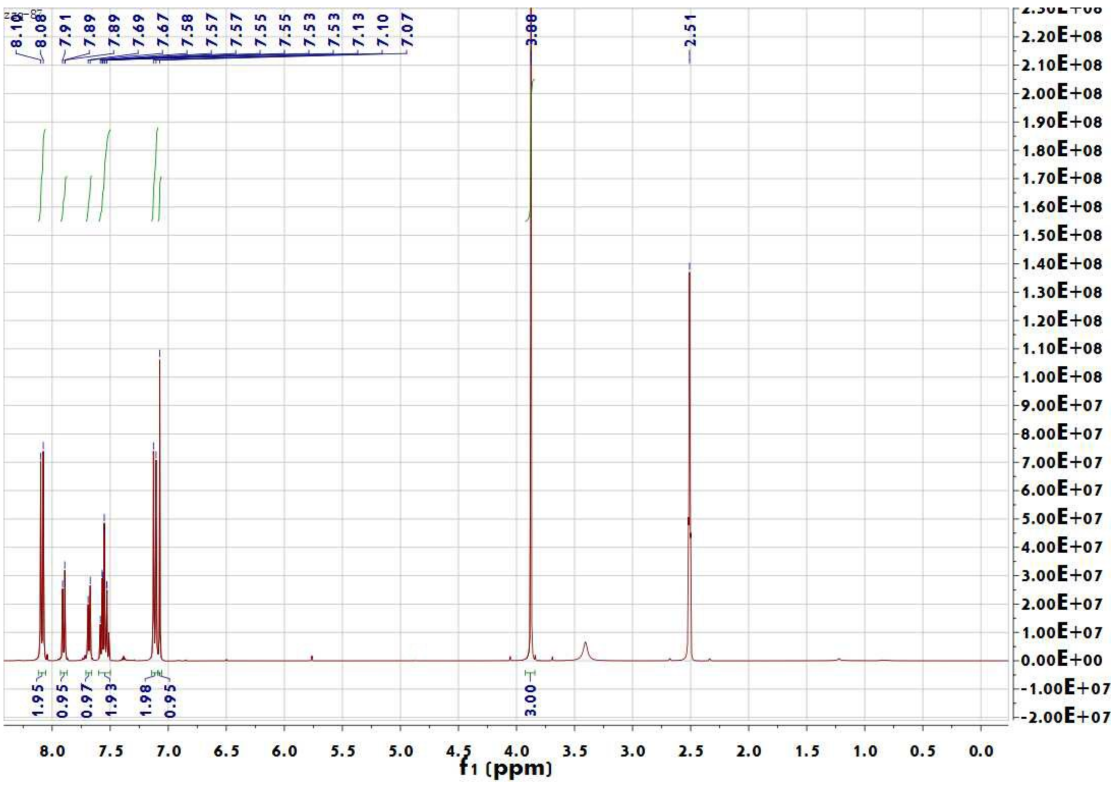

Figure S29. ^{1}H NMR (400 MHz) spectrum of compound **B4B** in DMSO-d_6

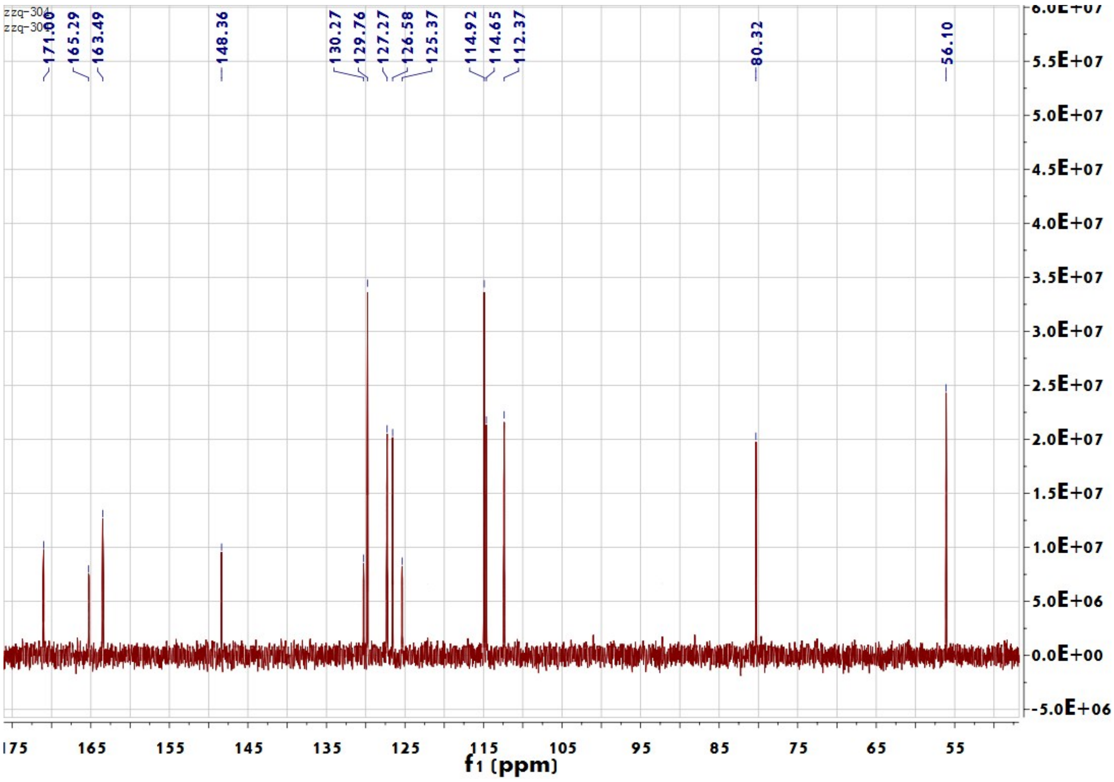

Figure S30. ^{13}C NMR (100 MHz) spectrum of compound **B4B** in DMSO-d_6

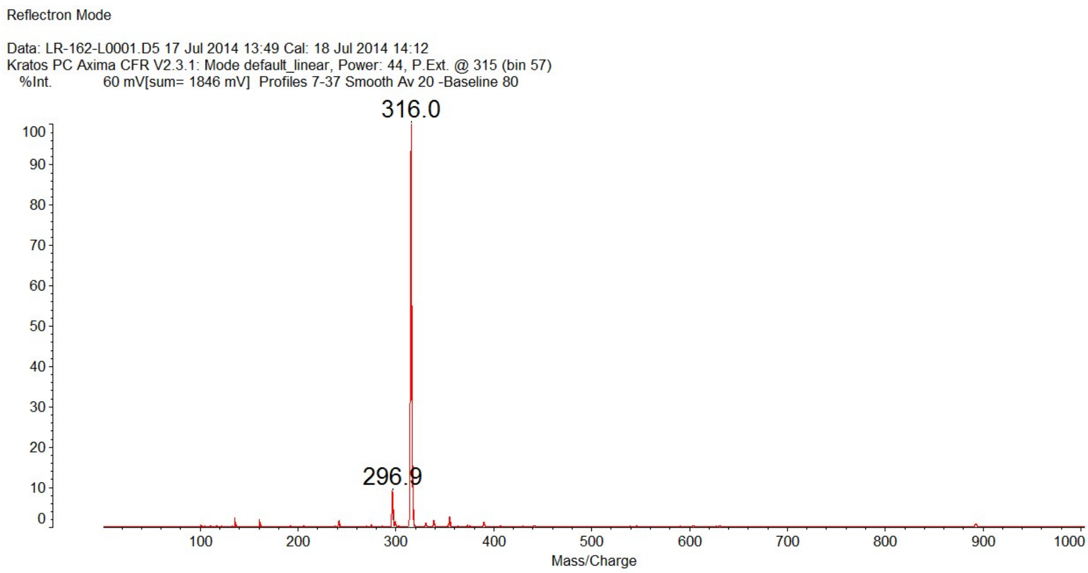

Figure S31. MALDI/TOF MS spectrum of compound **B4B**.

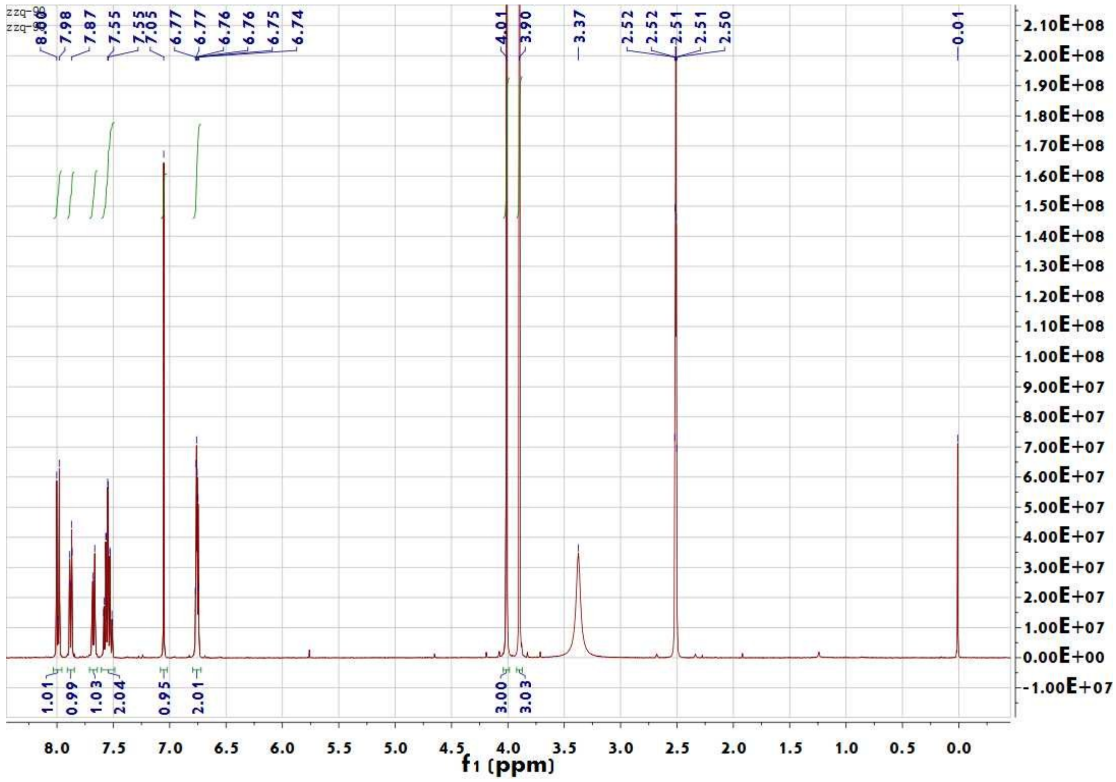

Figure S32. [1]H NMR (400 MHz) spectrum of compound **B24B** in DMSO-d_6

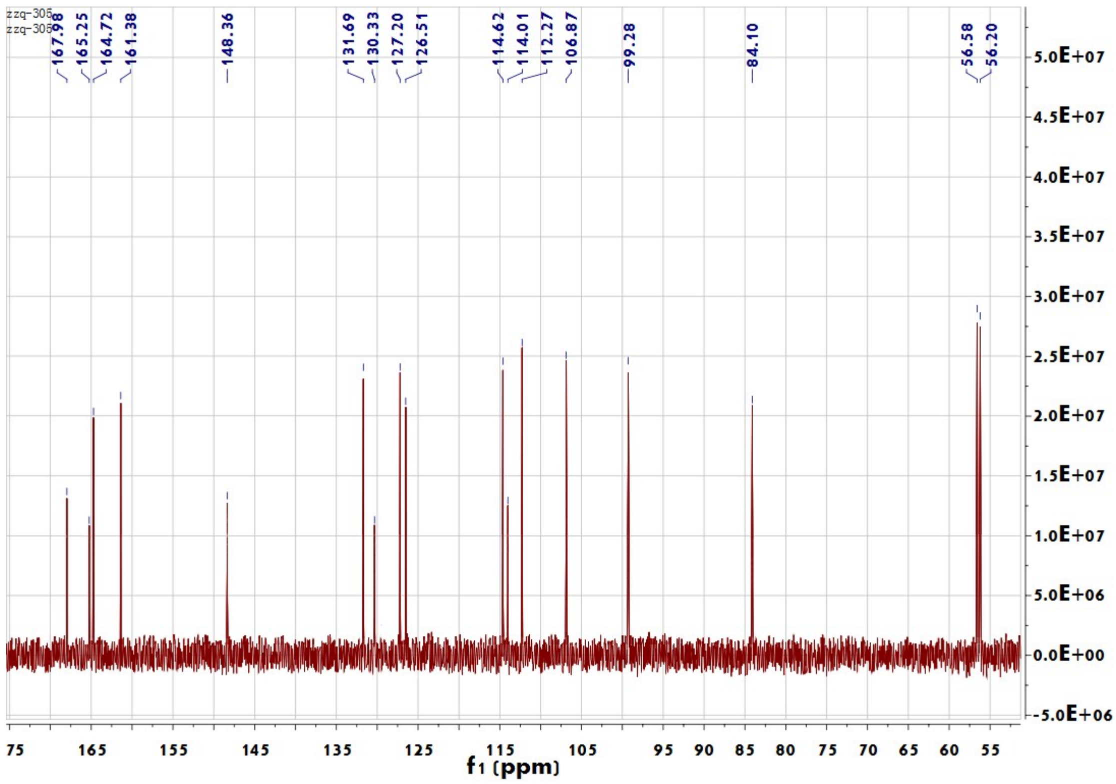

Figure S33. [13]C NMR (100 MHz) spectrum of compound **B24B** in DMSO-d_6

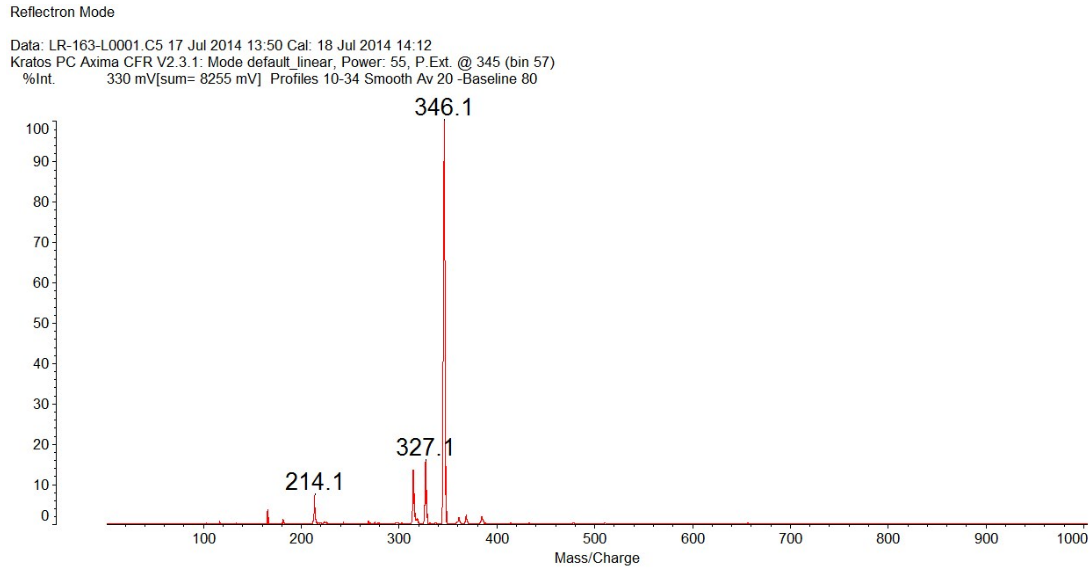

Figure S34. MALDI/TOF MS spectrum of compound **B24B**.

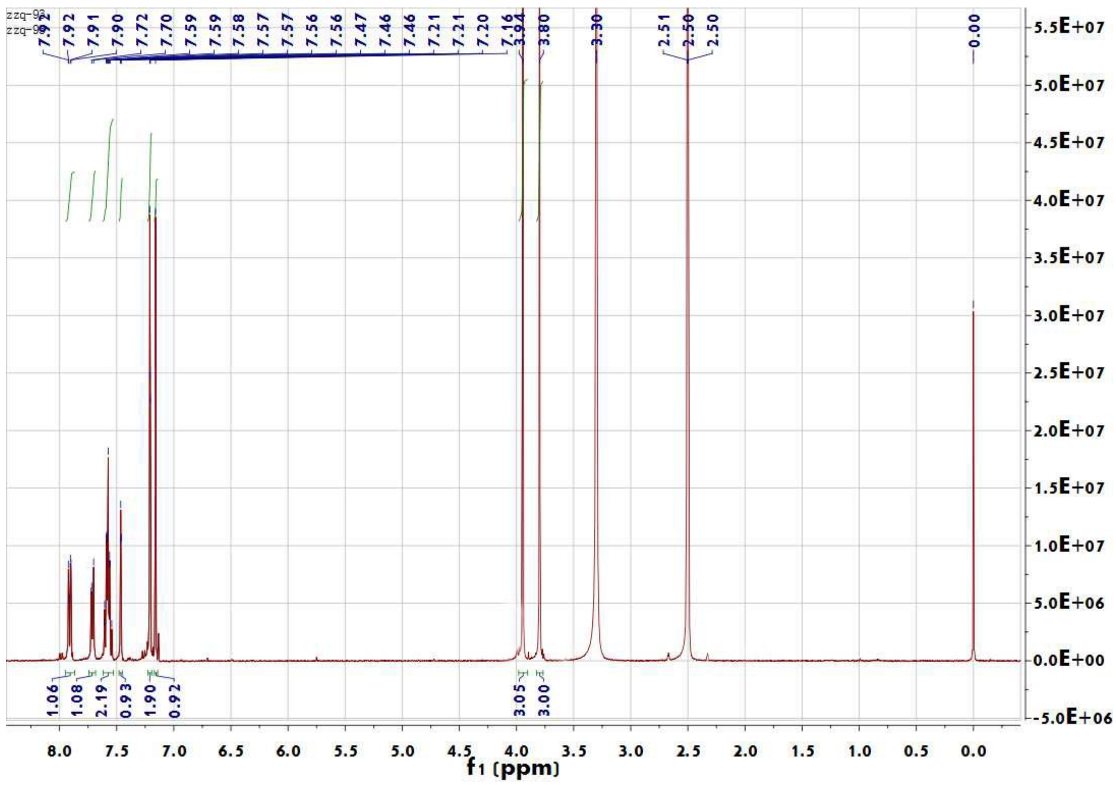

Figure S35. [1]H NMR (400 MHz) spectrum of compound **B25B** in DMSO-d_6

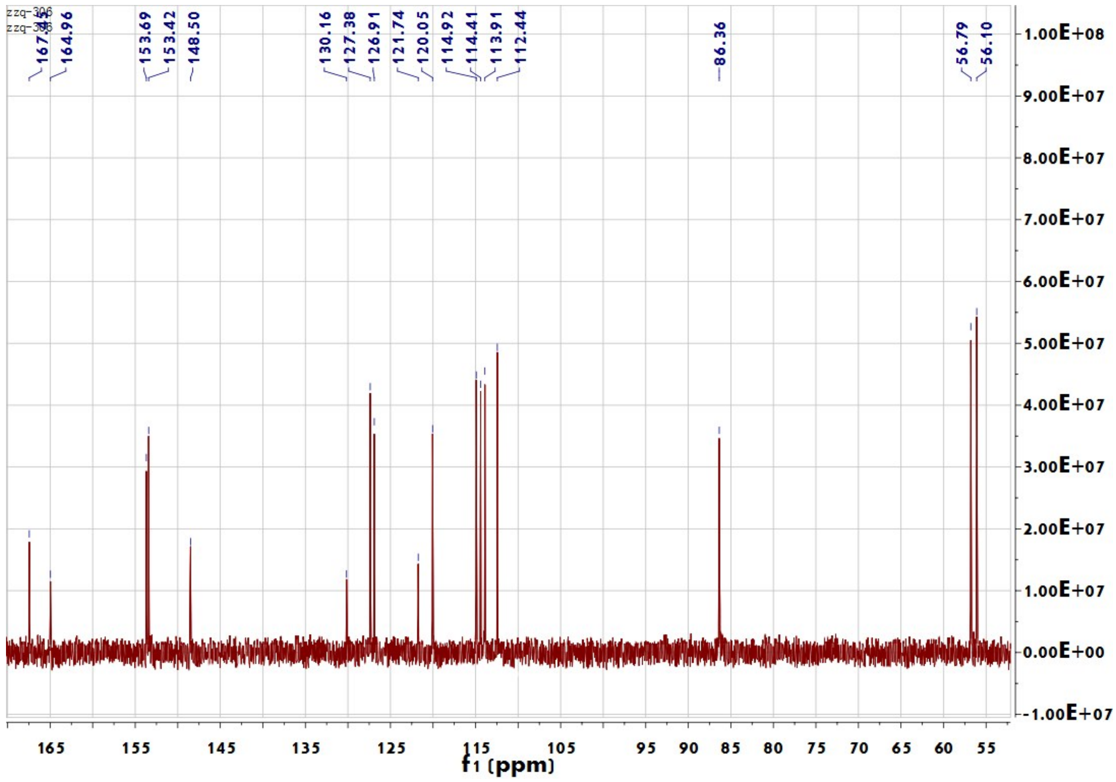

Figure S36. ^{13}C NMR (100 MHz) spectrum of compound **B25B** in DMSO-d_6

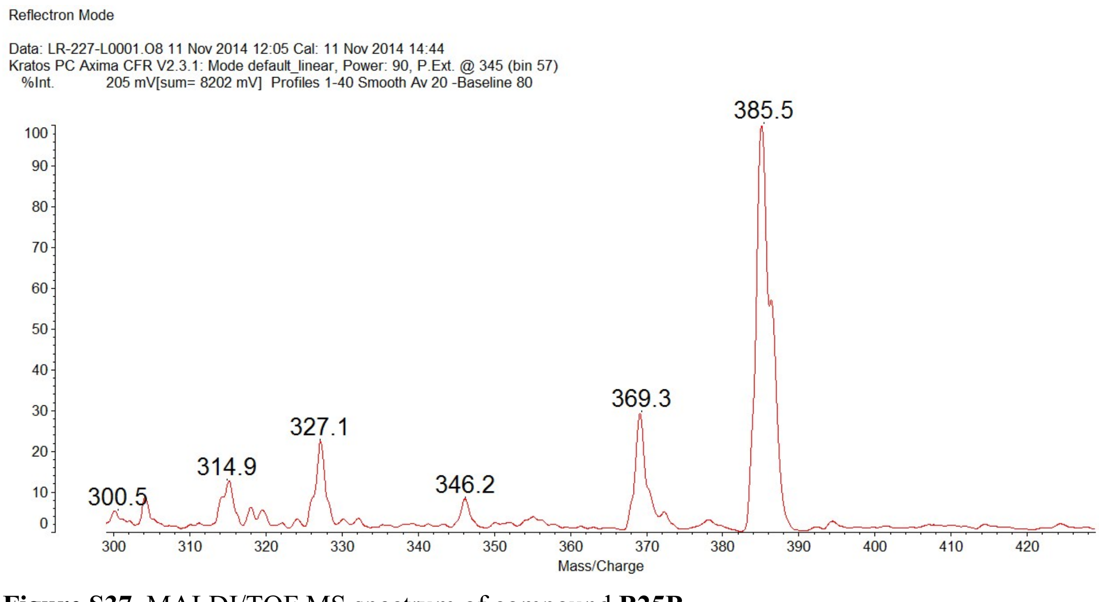

Figure S37. MALDI/TOF MS spectrum of compound **B25B**.

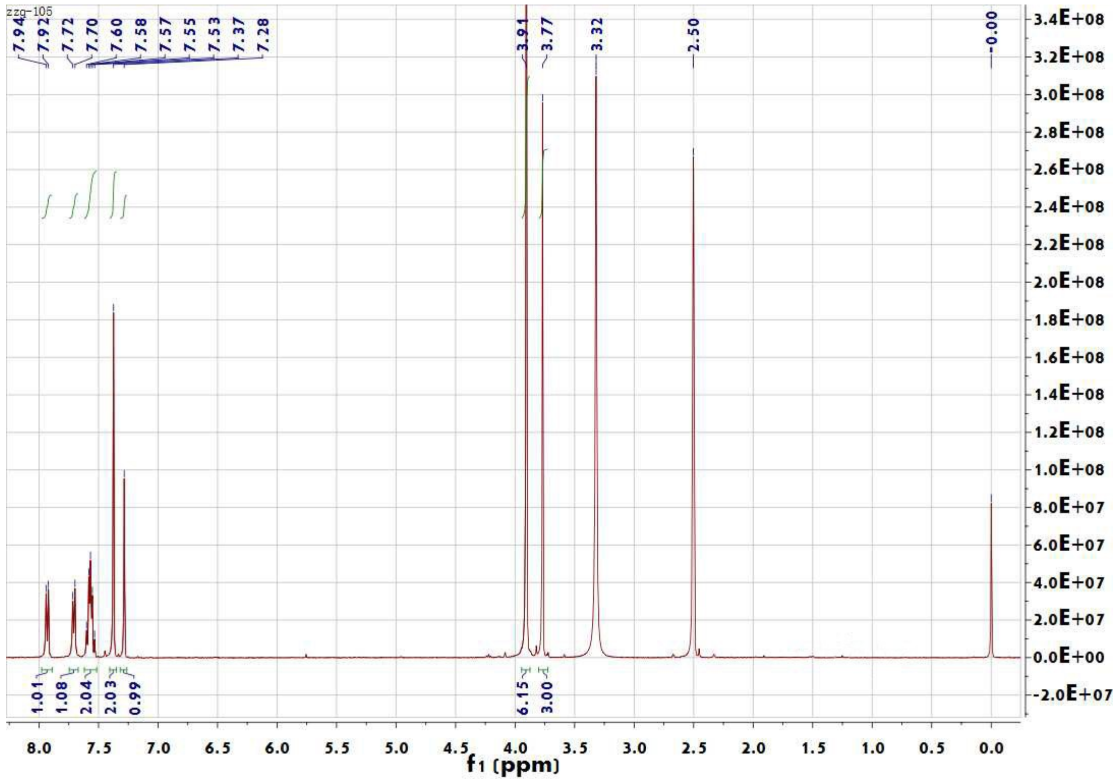

Figure S38. [1]H NMR (400 MHz) spectrum of compound **B345B** in DMSO-d_6

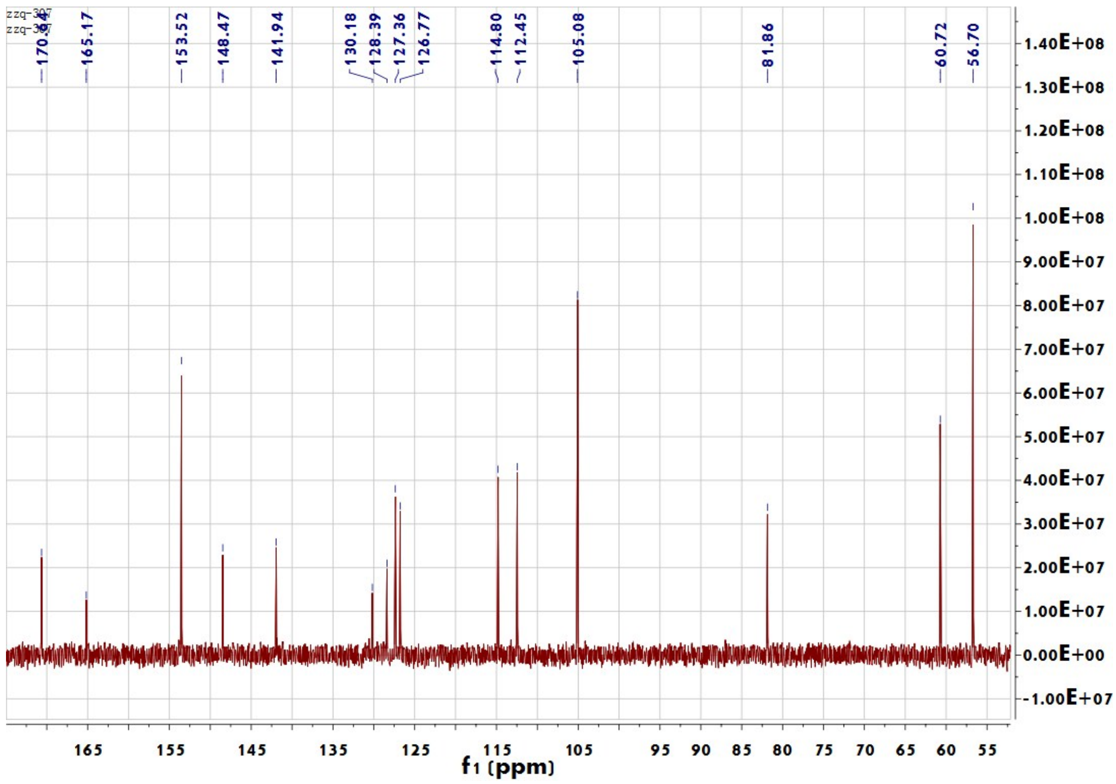

Figure S39. [13]C NMR (100 MHz) spectrum of compound **B345B** in DMSO-d_6

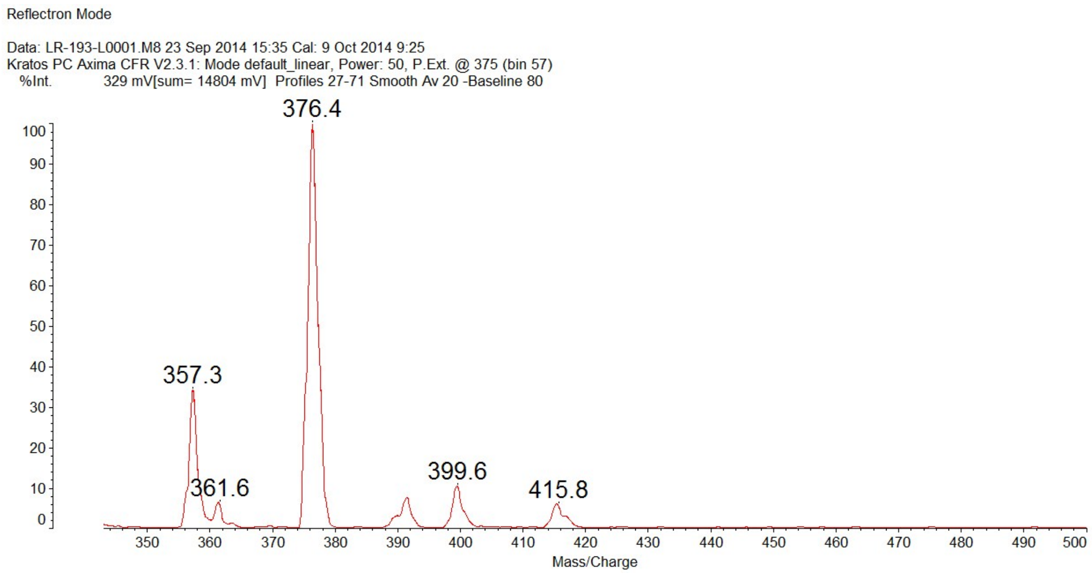

Figure S40. MALDI/TOF MS spectrum of compound **B345B**.